TAMPEREEN TEKNILLINEN YLIOPISTO
TAMPERE UNIVERSITY OF TECHNOLOGY

MUHAMMAD RIZWAN

PERFORMANCE EVALUATION OF WEARABLE ANTENNAS USING FLEXIBLE SUBSTRATES

Master of Science thesis

Examiner: Prof. Leena Ukkonen and Prof. Lauri Sydänheimo.
Examiner and topic approved by the Faculty Council of the Faculty of Computing and Electrical Engineering on 6th May 2015

ABSTRACT

Muhammad Rizwan: Performance Evaluation of Wearable Antennas Using Flexible Substrates.
Tampere University of technology
Master of Science Thesis, 54 pages, 00 Appendix pages
July 2015
Master's Degree Programme in Electrical Engineering
Major: Wireless Communications
Examiner: Professor Leena Ukkonen and Professor Lauri Sydänheimo

Keywords: Wearable Antennas, Circularly Polarized Antenna, Flexible Substrates, Wireless Body Area Network.

Body Area Network (BAN) is an expansion of Personal Area Networks (PANs) which enabled different devices to communicate with each other by placing them on human body. The applications of BAN include measuring run time physiological changes, foul playing detection in sports and navigation. We can also continuously keep the record of patient's health by monitoring the changes in human body. The frequency bands used in such systems are Industrial, Scientific and Medical (ISM) band (2.40 GHz to 2.50 GHz) and Wireless Body Area Network application band at 2.45 GHz. Wearable antennas are used as transceiver nodes in WBAN systems for sending and receiving the data or information. These antennas are kept flexible so that they do not hinder the movements of the human body. To make sure these antennas are flexible, different flexible materials are now-a-days used as substrates for the designing of the wearable antennas.

Due to the constant motion of human body, it is difficult to get the proper polarization alignment of the transceiver nodes for better power reception. Circular polarization (CP) operation eliminates the need to continuously align two nodes for receiving maximum power. Previously reported wearable antennas are mostly non-flexible, linearly polarized, large in size or have thick substrate which makes them difficult to be used in wearable applications.

In this thesis, two different flexible substrates have been used to design circularly polarized wearable antennas and their performance is analyzed near human body. The selected antenna type is micro-strip patch antenna with circular patch configuration operating for ISM band and WBAN applications at 2.45 GHz. To have a better idea of performance of flexible substrates, two substrates i.e. Denim and Ethylene Propylene Diene Monomer (EPDM) foam are selected having 1 mm and 3 mm thickness respectively. Copper tape with thickness 0.25 mm is used as conductive part for both the antennas. To achieve circular polarization a rectangular slot along the diagonal axis is inserted at the center of the circular patch. Performance of both antennas is analyzed in free space and in human body vicinity.

The antenna showed good agreement between simulated and measured free space results, however due to fabrication inaccuracies, some shifting of operating frequency is observed. EPDM antenna shows better results in terms of return loss, bandwidth and Axial Ratio (AR) compared with Denim antenna in free space. Free space bending is analyzed in two planes i.e. xz and yz, with two different bending radii (50 mm and 75 mm). Bending analysis showed that the performance of the antenna is affected more

when the antenna is bent along the direction which determines its resonance length. Impedance matching is improved when the antenna is bent in xz-plane. Beam width increases in the plane of bending which results in decreased antenna gain.

Human body is made up of 65-75 % water. The dielectric constant of water is very high (above 75 at 20°C) and at higher frequencies it absorbs power and can reduce the efficiency of any antenna placed nearby. The near body performance of the designed antennas is analyzed by varying the distance between the antenna and the human body using a polyethylene foam sheet of different thicknesses. Three different distances were selected i.e. 0 mm (directly on skin), 2 mm and 5 mm to have a better idea of the effects with respect to varying distance between the human body and the wearable antenna. The performance of the antenna in terms of the input matching and the impedance bandwidth is analyzed on two different body parts i.e. arm and leg, with bending in both xz-plane and yz-plane. The results show a decrease in return loss due to lossy nature of the human body, and increase in bandwidth due to the lowering of the Q factor of the antenna. The antenna gain is increased due to low penetration depth and reflections from the human body in simulation and real on-body measurements at high frequencies. The percentage increase in gain near human body for EPDM and Denim is around 19.56% and 10.66% respectively.

The summary of results shows that the designed antennas operate for desired frequency bands with good efficiency in all simulated and measured scenarios; however EPDM antenna is better in terms of antenna impedance and radiation characteristics, weight, wearing comfort, and can naturally and forcibly retract to its original dimensions after deformation. The copper tape used in fabricating the antenna peels off with time and makes the antenna less reliable. In future, the conductive part can be printed using Inkjet or Micro Dispense 3D Printer for a more reliable and accurate design of the wearable antenna.

PREFACE

The master thesis, “Performance Evaluation of Wearable Antennas Using Flexible Substrates” was done in partial fulfilment of the requirement for the Master of Science degree in Wireless Communications major, in the Department of Electronics and Communications Engineering at Tampere University of Technology. All the researches and investigations have been done in the Wireless Identification and Sensing Systems Research Group (WISE) under the supervision of Prof. Leena Ukkonen and Prof. Lauri Sydänheimo. I would like to thank my thesis examiners and supervisors, Prof. Leena Ukkonen and Prof. Lauri Sydänheimo, for all of their support, continuous guidance and for providing me an appropriate environment to complete my thesis. I am also thankful to all my colleagues in the WISE Group for their help and support.
I want to thank my friends specially Muhammad Waqas Ahmed Khan for his help during my measurements. I would like to thank my family for their continuous support to make this thesis possible.

Tampere, June 2015

Muhammad Rizwan

CONTENTS

1. INTRODUCTION 1
2. ELECTROMAGNETIC THEORY 2
2.1 Electric Field 2
2.2 Magnetic Field 2
2.3 Maxwell Equations 3
2.4 Wave Equations 3
2.5 Plane Wave 4
2.5.1 Linear Polarization 4
2.5.2 Circular Polarization 5
2.5.3 Elliptical Polarization 5
2.6 Transmission Line Theory 6
3. BASICS OF ANTENNA 8
3.1 Definition of Antenna 8
3.2 How is Radiation Accomplished? 8
3.3 Antenna Parameters 9
3.3.1 Input Impedance 9
3.3.2 Return Loss 9
3.3.3 Voltage Standing Wave Ratio 10
3.3.4 Bandwidth 10
3.3.5 Radiation Pattern 10
3.3.6 Beam width 11
3.3.7 Directivity and Gain 11
3.3.8 Polarization and Axial Ratio 12
3.3.9 Quality Factor 13
4. WEARABLE ANTENNAS 14
4.1 Body Area Networks 14
4.2 Literature Review of Wearable Antennas 15
4.3 Circularly Polarized Wearable Antennas 16
4.4 Need of Improvement in Wearable Antennas 18
5. CIRCULARLY POLARIZED WERABLE ANTENNA 19
5.1 Design of Denim Antenna 19
5.1.1 Effect of slot “s” on Return Loss 20
5.1.2 Effect of slot “s” on Axial Ratio 21
5.1.3 3D Radiation Pattern 21
5.1.4 Current Distribution on the Surface of Patch 22
5.2 Design of EPDM Antenna 22
5.2.1 Effect of slot “s” on Return Loss 23
5.2.2 Effect of slot “s” on Axial Ratio 23
5.2.3 3D Radiation Pattern 24

5.2.4 Current Distribution on the Surface of Patch 24
6. FREE SPACE MEASUREMENTS 26
6.1 Free Space Measurements of Denim Antenna 26
6.1.1 Bending Analysis of Denim Antenna 28
6.2 Free Space Measurements of EPDM Antenna 31
6.2.1 Bending Analysis of EPDM Antenna 34
7. ON-BODY MEASUREMENTS 38
7.1 Properties of Human Body 38
7.2 Need of On-body Measurements 38
7.3 On-body Measurements of Denim Antenna 39
7.3.1 Bending of Denim Antenna in xz-plane 39
7.3.2 Bending of Denim Antenna in yz-plane 40
7.4 On-body Measurements of EPDM Antenna 43
7.4.1 Bending of EPDM Antenna in xz-plane 43
7.4.2 Bending of EPDM Antenna in yz-plane 45
8. CONCLUSION AND FUTURE WORK 48
8.1 Conclusion 48
8.2 Future Work 49
9. PUBLICATIONS 50
REFERENCES 51

LIST OF FIGURES

Figure 2.1 *Linear Polarization (a) y-plane (b) x-plane.* 5
Figure 2.2 *Circular Polarization.* 5
Figure 2.3 *Elliptical Polarization (a) y-plane (b) x-plane.* 6
Figure 2.4 *Lumped-element equivalent circuit of a short transmission line [7].* 6

Figure 3.1 *Radiation Fields near an Antenna.* 8
Figure 3.2 *Radiation Pattern of Antenna with Different Lobes [11].* 11
Figure 3.3 *Axial Ratio in Circularly Polarized Wave.* 12

Figure 4.1 *Wearable Antenna (a) Structure (b) On human arm [14].* 15
Figure 4.2 *Circularly Polarized Antennas (a) Corner Truncated [22] (b) Probe Feed [23].* 16
Figure 4.3 *Circularly Polarized Antennas (a) Corner Truncated and Probe Feed [26] (b) Probe Feed with a Slot [27].* 17
Figure 4.4 *Circularly Polarized Antenna with Dual Feed [28].* 17
Figure 4.5 *Circularly Polarized Antennas (a) Corner Truncated (b) Corner Truncated with Slits [29].* 18

Figure 5.1 *Geometry of Denim Antenna (a) Front (b) Back.* 19
Figure 5.2 *Variation of Return Loss with slot "s".* 20
Figure 5.3 *Variation of Axial Ratio with slot "s".* 21
Figure 5.4 *3D Polar Plot at 2.45 GHz.* 21
Figure 5.5 *Current on the Surface of Patch at 2.45 GHz (a) 0° (b) 90° (c) 180°.* 22
Figure 5.6 *Geometry of EPDM Antenna (a) Front (b) Back.* 22
Figure 5.7 *Variation of Return Loss with slot "s".* 23
Figure 5.8 *Variation of Axial Ratio with slot "s".* 23
Figure 5.9 *3D Polar Plot at 2.45 GHz.* 24
Figure 5.10 *Current on the Surface of Patch at 2.45 GHz (a) 0° (b) 90° (c) 180°.* 24

Figure 6.1 *Free Space Measurement (a) VNA (b) Satimo Starlab.* 26
Figure 6.2 *Simulated and Measured Free Space Return Loss.* 26
Figure 6.3 *Simulated and Measured Free Space Axial Ratio.* 27
Figure 6.4 *Simulated and Measured Results for Gain and Axial Ratio at 2.45 GHz.* 27
Figure 6.5 *Simulated and Measured Efficiency.* 28
Figure 6.6 *Bending (a) xz 75mm (b) yz 75mm (c) xz 50mm (d) yz 50mm.* 29

Figure 6.7 Variation of Return Loss with Bending. 29
Figure 6.8 Variation of Axial Ratio with Bending. 30
Figure 6.9 Radiation Patterns. (a) xz-plane. (b) yz-plane..... 31
Figure 6.10 Environmental Adaptability of EPDM foam (a) In free space (b) On hand..... 32
Figure 6.11 Free Space Measurement (a) VNA (b) Satimo Starlab. 32
Figure 6.12 Simulated and Measured Free Space Return Loss. 33
Figure 6.13 Simulated and Measured Free Space Axial Ratio. 33
Figure 6.14 Simulated and Measured Results for Gain and Axial Ratio at 2.45 GHz..... 34
Figure 6.15 Simulated and Measured Efficiency..... 34
Figure 6.16 Bending (a) xz 75mm (b) yz 75mm (c) xz 50mm (d) yz 50mm. 35
Figure 6.17 Variation of Return Loss with Bending. 36
Figure 6.18 Variation of Axial Ratio with Bending. 36
Figure 6.19 Radiation Patterns (a) xz-plane. (b) yz-plane..... 37

Figure 7.1 Bending of Denim Antenna in xz-plane..... 39
Figure 7.2 Variation in Return Loss with Bending in xz-plane on the Arm. 40
Figure 7.3 Variation in Return Loss with Bending in xz-plane on the Leg. 40
Figure 7.4 Bending of Denim Antenna in yz-plane..... 41
Figure 7.5 Variation in Return Loss with Bending in yz-plane on the Arm. 41
Figure 7.6 Variation in Return Loss with Bending in yz-plane on the Leg. 42
Figure 7.7 Antenna Radiation Pattern near Human Body. 43
Figure 7.8 Bending of EPDM Antenna in xz-plane 43
Figure 7.9 Variation in Return Loss with Bending in xz-plane on the Arm. 44
Figure 7.10 Variation in Return Loss with Bending in xz-plane on the Leg. 44
Figure 7.11 Bending of EPDM Antenna in yz-plane. 45
Figure 7.12 Variation in Return Loss with Bending in yz-plane on the Arm. 46
Figure 7.13 Variation in Return Loss with Bending in yz-plane on the Leg. 46
Figure 7.14 Antenna Radiation Pattern near Human Body. 47

Figure 8.1 Problems in Copper Tape..... 49
Figure 8.2 Printers (a) Inkjet (b) Micro Dispense 3D. 49

LIST OF TABLES

Table 5.1 *Comparison of Denim and EPDM Antennas.* *25*

Table 6.1 *Change in Return Loss and Bandwidth of the Antenna with Bending.* *30*
Table 6.2 *Changes in Radiation Characteristics of the Antenna with Bending.* *31*
Table 6.3 *Change in Return Loss and Bandwidth of the Antenna with Bending.* *36*
Table 6.4 *Changes in Radiation Characteristics of the Antenna with Bending.* *37*

Table 7.1 *Properties of Human Body at 2.45 GHz [35].* *38*
Table 7.2 *Return Loss and Impedance Bandwidth for Bending in xz-plane.* *40*
Table 7.3 *Return Loss and Impedance Bandwidth in Bending along the yz-plane.* *42*
Table 7.4 *Antenna Gain Near Human Body.* *42*
Table 7.5 *Return Loss and Impedance Bandwidth in Bending along the xz-plane.* *45*
Table 7.6 *Return Loss and Impedance Bandwidth in xz-plane Bending.* *46*
Table 7.7 *Antenna Gain near Human Body.* *47*

LIST OF SYMBOLS AND ABBREVIATIONS

BAN	Body Area Network
PANs	Personal Area Networks
WBAN	Wireless Body Area Network
ISM	Industrial, Scientific and Medical
CP	Circular polarization
IEEE	Institute of Electrical and Electronics Engineers
VSWR	Voltage Standing Wave Ratio
dB	Decibel
HPBW	Half Power Beam Width
FNBW	First Null Beam Width
AR	Axial Ratio
PDA	Personal Digital Assistant
PIFA	Planar Inverted F Antenna
GSM	Global System for Mobile Communications
WLAN	Wireless Local Area Network
UMTS	Universal Mobile Telecommunications System
EPDM	Ethylene Propylene Diene Monomer
HFSS	High Frequency Structure Simulator
LHCP	Left Hand Circular Polarization
RHCP	Right Hand Circular Polarization
VNA	Vector Network Analyzer
FBR	Front to Back Ratio
N	Newton
C	Coulomb
Q	Electric Charge
B	Magnetic Flux Density
Wb	Weber
μ_o	Magnetic Permeability
J	Current Density
M	Magnetization Vector
μ	Permeability of the Medium
σ	Conductivity of the Material
γ	Complex Propagation Constant
ω	Angular Frequency of the Wave
E	Electric Field
H	Magnetic Field
Z	Impedance
R	Real
X	Imaginary
Γ	Reflection Coefficient
ρ	Voltage Standing Wave Ratio
F_{Upper}	Upper Cut off Frequency
F_{Lower}	Lower Cut off Frequency
$\theta_{beam\ width}$	Beam Width in Theta Plane
$\Phi_{beam\ width}$	Beam Width in Phi Plane
GHz	Giga Hertz
ε_r	Dielectric Constant

δ	Tangent Loss
Ω	Ohm
mm	Millimeter
%	Percentage
MHz	Mega Hertz
S/m	Siemens per meter

1. INTRODUCTION

Body Area Network (BAN) is an expansion of Personal Area Networks (PANs) that enabled devices to communicate with each other by implanting them on human body [1]. The applications of BAN include measuring run time physiological changes, foul playing detection in sports and navigation. We can also continuously keep the record of the patient's health by monitoring the changes in human body. The frequency bands used for Wireless Body Area Network (WBAN) applications are 2.45 GHz and Industrial, Scientific and Medical (ISM) band. Wearable antennas are used as a transceiver in WBAN systems to send and receive the data or information. These antennas are kept flexible so that they do not hinder the movements of human body. To make sure these antennas are flexible, different flexible materials are now-a-days used for the designing of the wearable antennas.

Due to the constant motion of human body, it is difficult to align the polarization of the transceiver nodes for better power reception. Circular polarization (CP) operation eliminates the need to continuously align two nodes for receiving maximum power [2][3]. Previously reported wearable antennas are mostly non-flexible [3], thick substrate [4], linearly polarized [3][4] or large in size [5] which makes them difficult to be used in wearable applications.

In this thesis, two different flexible substrates have been used to design circularly polarized wearable antennas and their performance is analyzed in bent state and near human body. In Chapter 2, the concepts of electromagnetic theory are explained while Chapter 3 covers the basics of an antenna. Chapter 4 includes the literature review and current state of art of a wearable antenna. Chapter 5 discusses the designing of a wearable antenna on two different substrates while Chapter 6 and 7 analyzes the performance of designed antennas in free space and near human body vicinity. Chapter 8 concludes the thesis and proposes future work that can be done related to the topic.

2. ELECTROMAGNETIC THEORY

The study of electromagnetic theory is necessary to understand antenna theory and wave propagation. In this chapter, the electromagnetic theory is explained with the help of Electric and Magnetic fields, Maxwell and Wave equations and some important concepts related to transmission lines.

2.1 Electric Field

Electric field (*V/m*) is defined as force (*N*) per unit charge (*C*). The strength of electric field is dependent on the amount of charge and distance from it. It is defined as,

$$E = \frac{F}{Q} = \frac{Q}{4\pi\varepsilon r^2}\hat{r} \tag{2.1}$$

where Q is the electric charge, ε is the electric permittivity of the medium and r is the distance from the electric charge.

The divergence and curl of electric field can be expressed by equations given below,

$$\nabla . E = \frac{\rho}{\varepsilon} \tag{2.2}$$

$$\nabla \times E = 0 \tag{2.3}$$

2.2 Magnetic Field

The magnetic flux density B (Wb/m^2) is defined using curl and divergence in magnetostatics due to time invariant currents. Equation 2.4 and 2.5 give the divergence and curl of magnetic flux,

$$\nabla . B = 0 \tag{2.4}$$

$$\nabla \times B = \mu_o J \tag{2.5}$$

where μ_o is the magnetic permeability of free space and J is the current density.

Magnetic field intensity H (A/m) can be computed using the relation mentioned in equation 2.6,

$$H = \frac{B}{\mu_o} - M = \frac{B}{\mu} \tag{2.6}$$

where M is the magnetization vector and μ is the permeability of the medium [6].

2.3 Maxwell Equations

Four Maxwell equations give the relation between electric field, magnetic field, electric charge and electric current. These equations describe how the electric and the magnetic field are generated and affected by each other and by current and charges. These four equations are the fundamental laws known as Faraday's law of induction (2.7), Ampere's circuital law (2.8), Gauss's law for electric fields (2.9) and Gauss's law for magnetic fields (2.10) [7],

$$\nabla \times E = -\frac{\partial B}{\partial t} - M \tag{2.7}$$

$$\nabla \times H = \frac{\partial D}{\partial t} + J \tag{2.8}$$

$$\nabla . D = \rho \tag{2.9}$$

$$\nabla . B = 0 \tag{2.10}$$

The current density in equation 2.8 can be calculated using equation 2.11,

$$J = \sigma E \tag{2.11}$$

where σ is the conductivity of the material.

2.4 Wave Equations

Maxwell's equations are given in phasor form when dependency of electric and magnetic fields is on time ($e^{j\omega t}$) [7].

$$\nabla \times \bar{E} = -j\omega\mu\bar{H} \tag{2.12}$$

$$\nabla \times \bar{H} = j\omega\varepsilon\bar{E} + \sigma\bar{E} \tag{2.13}$$

Helmholtz equations (2.16) and (2.17) can be derived by taking curl of equations (2.12), (2.13) and by using the vector calculus identity in equation (2.15) [7].

$$\nabla \times \nabla \times \bar{E} = -j\omega\mu\nabla \times \bar{H} = \omega^2\mu\varepsilon\bar{E} \tag{2.14}$$

$$\nabla \times \nabla \times A = \nabla(\nabla . A) - \nabla^2 A \tag{2.15}$$

$$\nabla^2\bar{E} + \omega^2\mu\varepsilon\left(1 - j\frac{\sigma}{\omega\varepsilon}\right)\bar{E} = \nabla\left(\frac{\rho}{\varepsilon}\right) \tag{2.16}$$

$$\nabla^2\bar{H} + \omega^2\mu\varepsilon\left(1 - j\frac{\sigma}{\omega\varepsilon}\right)\bar{H} = 0 \tag{2.17}$$

The phasor domain and time domain representation of above mentioned equations in source free medium for one dimension are given in equation (2.18) and (2.19).

$$E(z) = E^{+}e^{-\gamma z} + E^{-}e^{\gamma z} \tag{2.18}$$

$$E(z,t) = Ee^{-\alpha z}\cos(\omega t - \beta z) \tag{2.19}$$

where γ is the complex propagation constant for the medium and can be expressed by equation (2.20) [7],

$$\gamma = \alpha + j\beta = j\omega\sqrt{\mu\varepsilon}\sqrt{\alpha - j\frac{\sigma}{\omega\varepsilon}} \tag{2.20}$$

2.5 Plane Wave

When E field is in the same direction, the same value and the same phase in the plane perpendicular to the direction of propagation, it is called a plane wave. The definition is same for H field as well. E and H are perpendicular to each other in a propagating wave. When a plane wave propagates in a loss-less medium, there is no loss and amplitude of wave remains constant i.e. α=0 and γ is imaginary. If the medium is a lossy dielectric, then conductivity is σ=0 but permittivity ε of the medium is complex, hence there will be some attenuation faced by the wave i.e. $\alpha \neq 0$ and the amplitude keeps on decreasing while the wave propagates. The conductor losses in a medium can be expressed using skin depth.

$$\delta_s = \frac{1}{\alpha} = \sqrt{\frac{2}{\omega\mu\sigma}} \tag{2.21}$$

where ω is the angular frequency of the wave. If the propagation medium is a perfect conductor the EM wave cannot propagate inside and is reflected back [7].

The polarization of the EM wave is the orientation of E field and is divided into three categories [8].

2.5.1 Linear Polarization

In linear polarization E field vector varies only in one plane. The plane can be either in x-plane or y-plane. Axial Ratio (AR) is defined as the ratio of the major axis to the minor axis. In case of linear polarization, the AR is infinity (∞) [8].

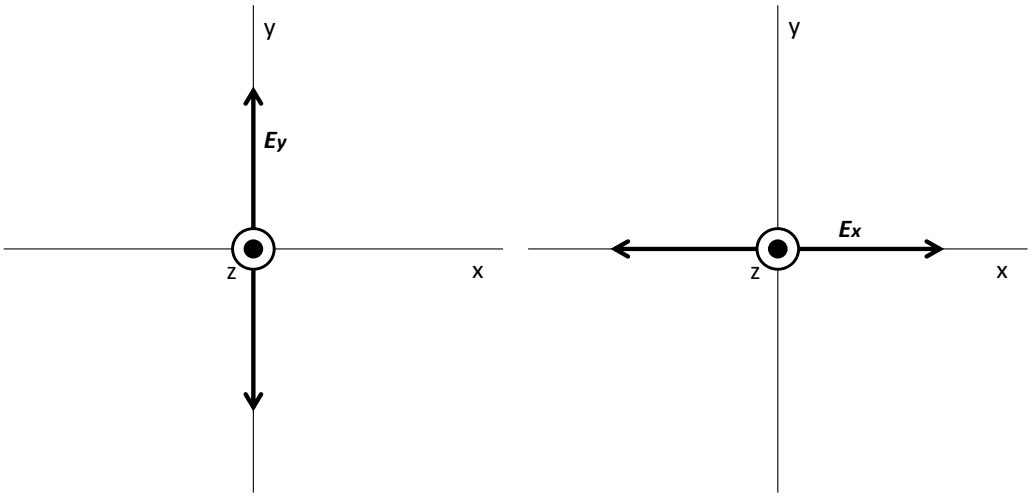

(a) (b)

Figure 2.1 *Linear Polarization (a) y-plane (b) x-plane.*

2.5.2 Circular Polarization

In circular polarization *E* field vector varies in two planes with equal magnitude. In case of circular polarization, the AR is 1 [8].

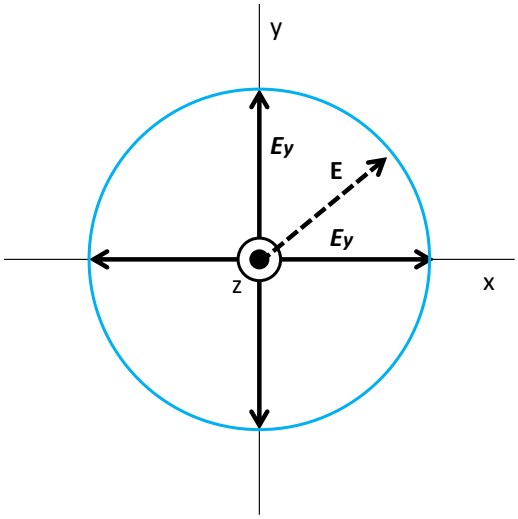

Figure 2.2 *Circular Polarization.*

2.5.3 Elliptical Polarization

In elliptical polarization *E* field vector varies in two planes with different magnitude. In case of elliptical polarization, the AR is dependent on the magnitude of both vectors and varies between 1 to infinity (∞) [8].

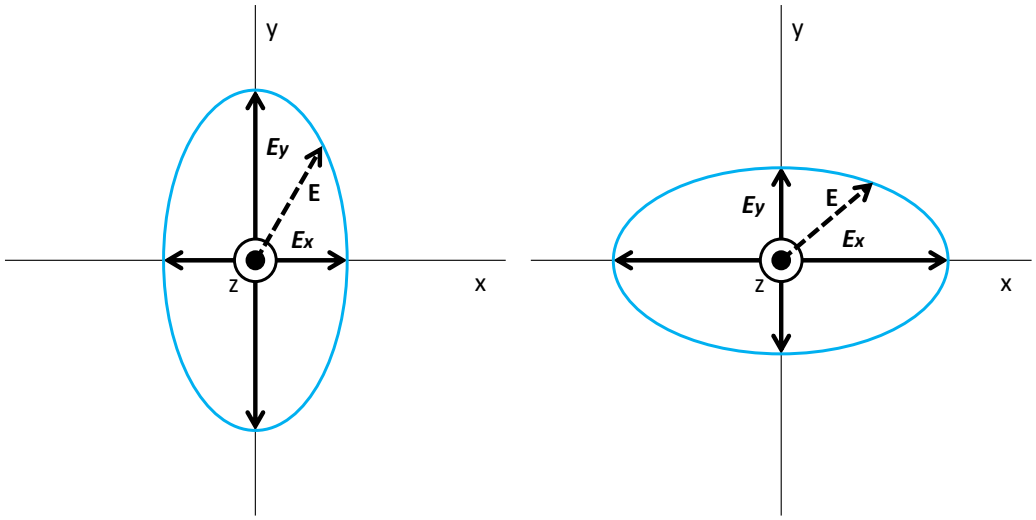

(a) (b)

Figure 2.3 *Elliptical Polarization (a) y-plane (b) x-plane.*

2.6 Transmission Line Theory

Transmission line theory is used when the physical dimensions of the network are comparable to the wavelength of the signal. Figure shows the Lumped-element equivalent circuit of a short transmission line [7].

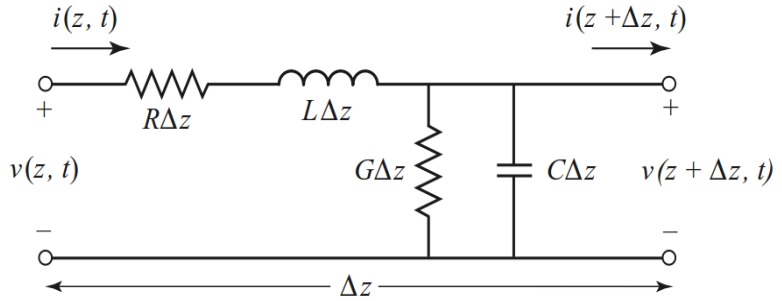

Figure 2.4 *Lumped-element equivalent circuit of a short transmission line [7].*

In order to find the voltage and current in the circuit, we can use the wave equation and write them as follows,

$$V(z) = V_o^+ e^{-\gamma z} + V_o^- e^{\gamma z} \tag{2.22}$$

$$I(z) = I_o^+ e^{-\gamma z} + I_o^- e^{\gamma z} \tag{2.23}$$

where γ is the complex propagation constant given by the formula [7],

$$\gamma = \alpha + j\beta = \sqrt{(R + j\omega L)(G + j\omega C)}$$

R = Series Resistance per unit Length, for both conductors, in Ω/m.
L = Series Inductance per unit Length, for both conductors, in H/m.
G = Shunt Conductance per unit Length, in S/m.
C = Shunt Capacitance per unit Length, in F/m.

The impedance of the line can be written as [7],

$$Z_o = \frac{V_o^+}{I_o^+} = \frac{V_o^-}{I_o^-} = \sqrt{\frac{(R + j\omega L)}{(G + j\omega C)}} \tag{2.24}$$

Whenever a transmission line is not matched, reflections will occur. The reflection coefficient in terms of reflected voltages is defined as [7],

$$\Gamma = \frac{V_o^-}{V_o^+} = \frac{Z_L - Z_o}{Z_L + Z_o} \tag{2.25}$$

The reflected waves super position on the incident wave and create a standing wave when $Z_L \neq Z_o$. These standing waves are described using a parameter known as Standing Wave Ratio (SWR) given by equation [7],

$$SWR = \frac{V_{max}}{V_{min}} = \frac{1 + |\Gamma|}{1 - |\Gamma|} \tag{2.26}$$

3. BASICS OF ANTENNA

This chapter discusses the definition of an antenna and the parameters used to evaluate an antenna. These parameters are necessary to characterize the behavior of an antenna and its types.

3.1 Definition of Antenna

An antenna is an essential component of a communication system [9]. It is used to send or receive radio waves. According to IEEE definition, antenna is defined as [10]:

"That part of a transmitting or receiving system that is designed to radiate or receive radio waves".

According to Webster's Dictionary in [11], antenna is defined as:

"It is usually a metallic device (as a rod or wire) for transmitting or receiving waves".

In general, antenna is a passive component that can transmit and receive electromagnetic energy from the space surrounding it in order to establish a wireless connection between two or more devices. Antennas are reciprocal devices i.e. they have the same kind of properties whether in transmit or in receive mode.

3.2 How is Radiation Accomplished?

To produce time varying *E* and *H* fields in antenna, we need to create time-varying current or an acceleration (or deceleration) of charges. When these two conditions are met, the antenna will radiate in all directions [8][11]. The radiation field near an antenna can be divided into three regions that are reactive near field, radiating near field (Fresnel Zone) and far field (Fraunhofer Zone) [11]. Figure 3.1 shows the radiation fields near an antenna.

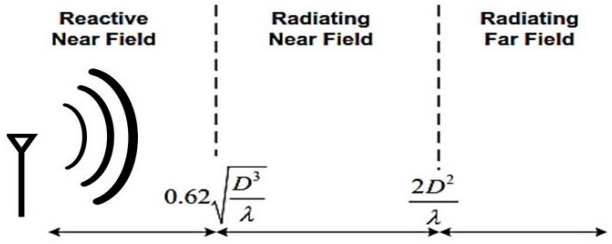

Figure 3.1 *Radiation Fields near an Antenna.*

The immediate vicinity of the antenna where the reactive field predominates is called the reactive near field. Generally, the reactive near field of the antenna is at a distance $R < 0.62\sqrt{\frac{D^3}{\lambda}}$ from the antenna surface, where λ is the wavelength and D is the largest dimension of the antenna [11]. The radiating near field or Fresnel region is the region between the near and the far fields. In this region, the reactive fields do not dominate and angular field distribution is dependent upon the distance from the antenna. The range of the radiating near field is $0.62\sqrt{\frac{D^3}{\lambda}} < R < \frac{2D^2}{\lambda}$ [11]. The far field is the most important region around the antenna. In this region, the radiation pattern does not change shape with distance and a propagating wave can be assumed as a plane wave. The far field region starts from $R > \frac{2D^2}{\lambda}$ and extends away from the antenna [11].

3.3 Antenna Parameters

Antennas have some important parameters which need to be considered while designing them. This section discusses all the fundamental parameters of the antenna along with their suitable values.

3.3.1 Input Impedance

The input impedance of an antenna is defined as the ratio of the voltage current at the terminals of the antenna. The real part of the antenna impedance represents power that is either radiated away or absorbed within the antenna. The imaginary part of the impedance represents power that is stored in the near field of the antenna. The antenna having real impedance resonates [7].

$$Z_A = R_A + jX_A \tag{3.1}$$

3.3.2 Return Loss

The input impedance of the antenna should be matched to the source impedance. If both the impedances are not matched then some part of the transmitted power will be reflected back. This reflected power relative to input or incident power is called the return loss of the antenna. In general, the threshold for return loss is -10 dB which means 90% of incident power should be transmitted. The antenna having better matching will have more than 90% of incident power transmitted.

$$RL(dB) = -20\log|\Gamma| \tag{3.2}$$

where, Γ is the reflection coefficient [7][11].

3.3.3 Voltage Standing Wave Ratio

The Voltage Standing Wave Ratio is defined as the measure of impedance mismatch between the load and the transmission line. VSWR can also be defined as the ratio of maximum voltage to minimum voltage [8].

$$VSWR(\rho) = \frac{V_{\max}}{V_{\min}} \tag{3.3}$$

In terms of reflection coefficient, VSWR can be written as,

$$VSWR(\rho) = \frac{1+\Gamma}{1-\Gamma} \tag{3.4}$$

Ideally the value of VSWR should be 1 but in antenna designing, VSWR less than 2 is considered as acceptable.

3.3.4 Bandwidth

The Bandwidth of the antenna is defined as the range of frequencies in which antenna operates. The range of frequency is the difference between the upper cut-off frequency and lower cut-off frequency. Percentage bandwidth can be written as [8],

$$BW(\%) = \frac{2\times\left(F_{Upper} - F_{Lower}\right)}{F_{Upper} + F_{Lower}} \tag{3.5}$$

3.3.5 Radiation Pattern

A radiation pattern is a graphical representation of the field strength transmitted or received by the antenna. The radiation pattern of antenna can be divided into two fundamental planes, i.e. *E* plane and *H* plane, containing the *E* field and the *H* field vectors. The radiation pattern is usually plotted on a logarithmic scale or more commonly in decibels (dB).

The radiation pattern of antenna can also be divided into different lobes [11]. The major or main lobe is that portion of the radiation pattern which contains the maximum power. Any lobe other than the major lobe is called the minor lobe. Mostly the minor lobe consists of the side lobes and the back lobes. Side lobes are close to the main lobe but contain less power than it, while the back lobe is opposite to the major lobe or make an an-

gle of 180º with the major lobe. Figure 3.2 shows the radiation pattern of an antenna with different lobes.

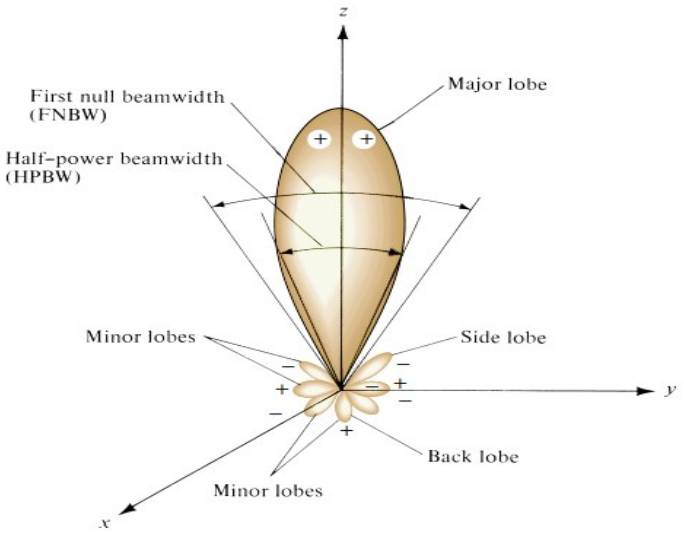

Figure 3.2 *Radiation Pattern of Antenna with Different Lobes [11].*

3.3.6 Beam width

The Beam width of the antenna is defined as the angular width where the radiated power becomes half the maximum power or is reduced by 3 dB. It is measured in radians or degrees. Beam width or Half Power Beam Width (HPBW) is actually the same thing. Another type of beam width is the First Null Beam Width (FNBW) which is the angular width measured between the first nulls on the major lobe. Figure 3.2 shows the HPBW and FNWB in the major lobe.

3.3.7 Directivity and Gain

The Directivity is the measure of power an antenna radiates in a particular direction as compared to its radiation in any other direction. It is equal to the power gain if the antenna is 100% efficient. Directivity can also be defined in terms of maximum power density and average value using the following relation [11],

$$D = \frac{P_{\max}}{P_{average}} \tag{3.6}$$

Directivity in terms of beam width is calculated using the following approximation [11],

$$D \approx 4\pi \frac{\left(\frac{180}{\pi}\right)^2}{\phi_{beamwidth} \times \varphi_{beamwidth}} \approx \frac{41253}{\phi_{beamwidth} \times \varphi_{beamwidth}} \tag{3.7}$$

Gain or power gain shows how efficiently the available power at input terminals of antenna is transmitted. The unit of gain is dB; if taken considering the isotropic antenna then it is represented in dBi. Gain and directivity are related to each other by the efficiency of the antenna [11].

$$G = kD \tag{3.8}$$

where k is antenna efficiency.

3.3.8 Polarization and Axial Ratio

Polarization is the orientation of electromagnetic fields radiated by an antenna. As explained in Chapter 2, polarization can be of three types i.e. linear, circular and elliptical.

Axial Ratio (AR) is defined as the ratio of the major axis to the minor axis [11].

$$AR = \frac{Major\ axis}{Minor\ axis} = \frac{OA}{OB} \tag{3.9}$$

The main focus of this thesis is to design a circularly polarized antenna. Figure 3.3 shows the circularly polarized wave. Note that in circular polarization, the major axis is equal to the minor axis.

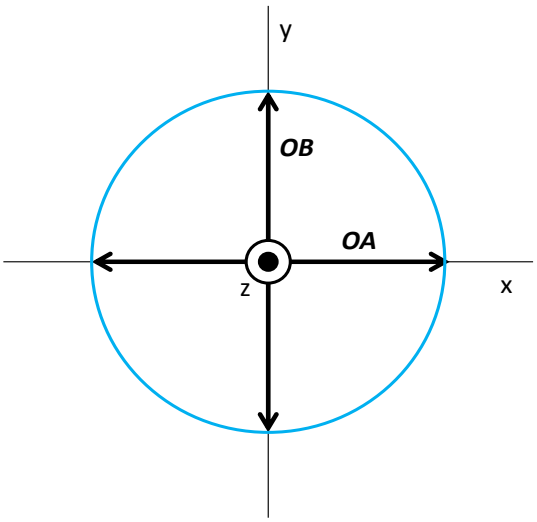

Figure 3.3 *Axial Ratio in Circularly Polarized Wave.*

AR is mostly measured in the decibel scale and the ideal value is 0 dB for circularly polarized fields. However, in designing, the value of AR less than 3 dB for any antenna is considered to generate a circularly polarized wave.

3.3.9 Quality Factor

The Quality factor of an antenna relates the radiated energy P_R and ohmic losses P_L of an antenna to the reactive energy P_S stored around it [7].

$$Q(\omega) = \frac{\omega P_S(\omega)}{P_R(\omega) + P_L(\omega)} \tag{3.10}$$

The quality factor of an antenna is inversely related to its bandwidth. Microstrip patch antennas have narrow bandwidth due to the high quality factor.

4. WEARABLE ANTENNAS

This chapter discusses the need for wearable antennas in recent technology and their brief history. Different sections of the chapter include details of BAN, literature review of the wearable antennas and current state of the art of circularly polarized wearable antennas.

4.1 Body Area Networks

IEEE 802.15 defines Body Area Network (BAN) as:

"A communication standard optimized for low power devices and operation on, in or around the human body (but not limited to humans) to serve a variety of applications including medical, consumer electronics / personal entertainment and other" [12].

A BAN system consists of various nodes attached to different body parts. These nodes are responsible for communicating with each other and transmitting the data to any remote server [12]. A node is subdivided into a sensor, an actuator and a Personal Digital Assistant (PDA). The sensor is the most important part and it includes a memory unit for data storage and an antenna for transmitting and receiving the collected data [13].

The antennas used in BAN systems must fulfill the following conditions:

1. Compact and light weight.
2. Flexible and retain their shape.
3. Radiation away from the human body.
4. Stable characteristics in the human body vicinity.

Keeping in mind the above conditions for the antennas in BAN systems, at the end of 20^{th} century, researchers invented wearable antennas that can efficiently operate near human body vicinity without hindering its movements.

The characteristics of wearable antennas are compact size, light weight, flexible, cost effective and robust. Traditional antennas that were non-flexible were difficult to integrate into BAN systems compared with the flexible wearable antennas. These advantages made them become the latest research area in antenna designing [12].

4.2 Literature Review of Wearable Antennas

The research work done on wearable antennas includes different antenna types like microstrip patch antenna and PIFA antenna etc. Different shapes of patches were used which included E-shape and U-slot patch antennas. In 1999, the first research work on wearable antennas was published which was based on a dual band planar antenna designed for GSM and Bluetooth 2.4 GHz band applications [14]. A U-slot was used to achieve dual band operation in the antenna and the possible placement for the antenna on the human body was on the sleeve. The antenna was fabricated on a rigid substrate but still due to its size and placement on human body, it was considered as a wearable antenna. To minimize the effect of the human body the author used a ground plane.

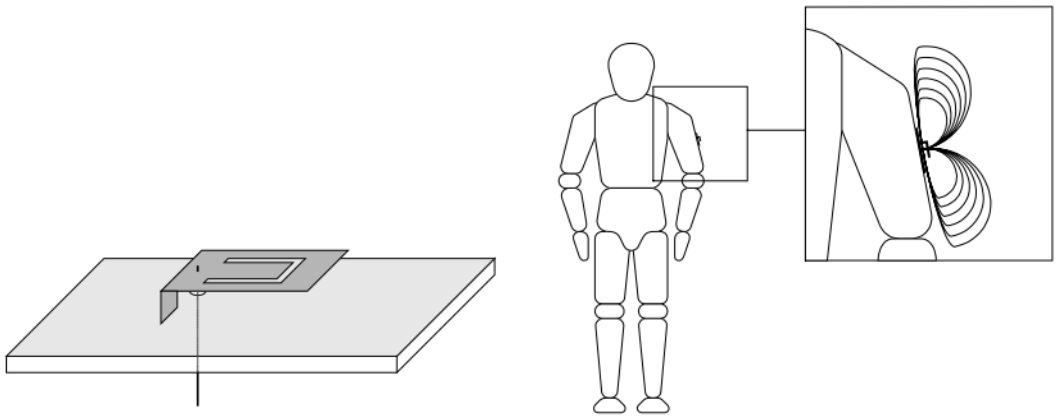

(a) (b)

Figure 4.1 *Wearable Antenna (a) Structure (b) On human arm [14].*

The wearable antenna technology became a hot topic after the research work done in 1999 and many researchers started working on it. A new type of wearable antenna was introduced in 2001 in which fabric was used as substrate so that the antenna can be comfortable to wear [15]. In 2002, a flexible printed IFA antenna for 2.4 GHz WLAN and UMTS 2.1 GHz was designed for application of smart clothing [16]. These fabric based antennas were characterized as a sub domain of wearable antennas known as textile antennas. A fleece fabric antenna working for 2.45 GHz WLAN band was introduced in 2003 for emergency worker's clothing [17]. The effect of bending in the wearable antenna was studied at 2.5 GHz in 2003 [18].

New applications for wearable antennas were introduced from 2003-2007 including military and safety measures [19][20]. Different types of substrates and conductive clothes were used in designing the wearable antenna i.e. electro textiles. The electrical properties of electro textiles were studied separately to have a better conductive and less resistive material. The use of electro textiles introduced embroidered antennas where conductive threads are used in the sewing of the antennas.

The applications of the wearable antenna operate near human body so it was necessary to characterize the performance of the antenna near human body. In 2004, a detailed analysis of antenna performance near human body was presented [21]. The antenna performance was analyzed near upper part of human chest and arm. The results showed that the antenna can operate near human body with sufficient return loss.

Initially, the designed wearable antennas were linearly polarized but in 2004 circularly polarized wearable antennas were introduced.

4.3 Circularly Polarized Wearable Antennas

The first research work related to circularly polarized wearable antennas was presented in 2004 [22]. Corner truncation was used to achieve circular polarization. Probe feeding along the diagonal of the patch of the antenna was used to achieve circular polarization in 2006 [23]. Location of the feed point is very important in achieving circular polarization. Textile Antenna for Off-Body Communication for fire fighters used optimized feed point to have good matching and circular polarized radiation characteristics [24][25].

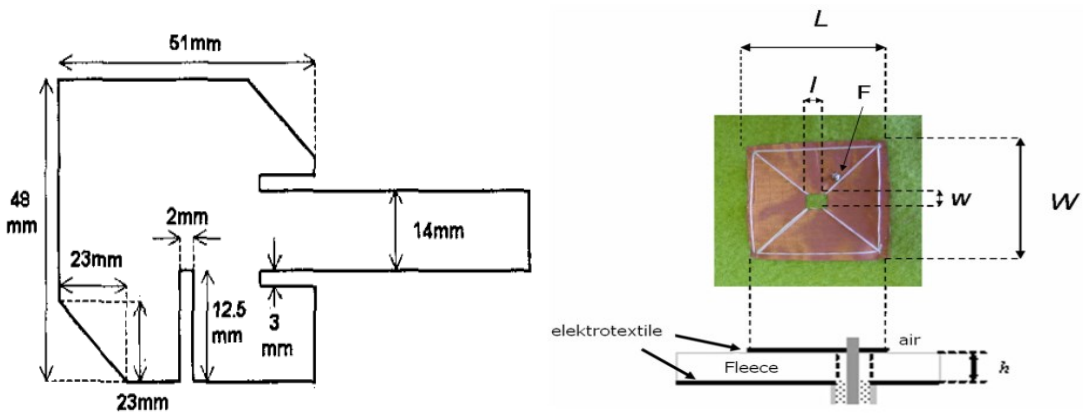

(a) (b)

Figure 4.2 *Circularly Polarized Antennas (a) Corner Truncated [22] (b) Probe Feed [23].*

The same probe feeding technique was used in some other research work. Another important thing to note here is that most of the designed antennas were simple structures with no optimization and used large radiating area [26][27].

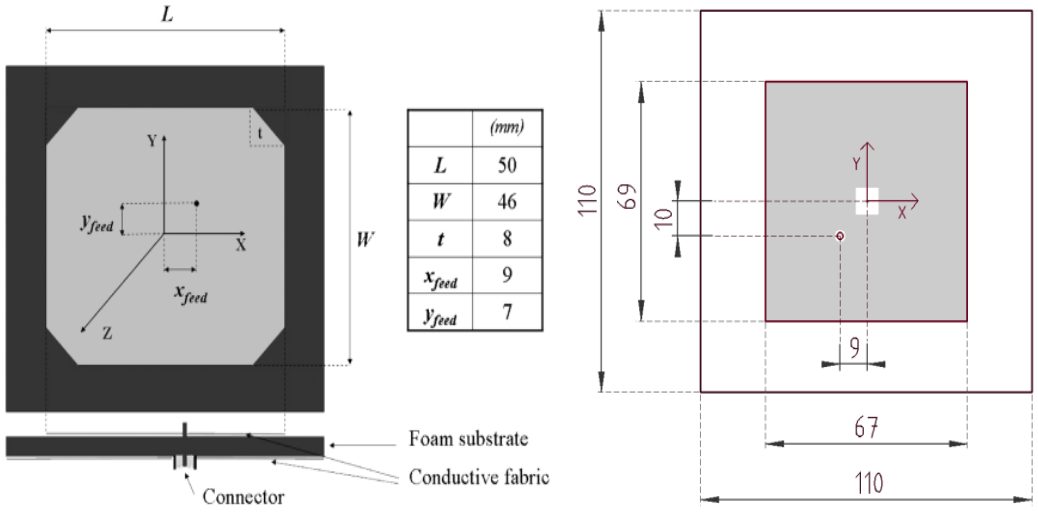

(a) (b)

Figure 4.3 *Circularly Polarized Antennas (a) Corner Truncated and Probe Feed [26] (b) Probe Feed with a Slot [27].*

Polarization mismatch of wearable antennas were studied in the research work published in 2013 [28]. The main drawback of this work was that the antennas were designed on rigid substrate. To achieve circular polarization dual feed transmission line was used. The current fed using one line will be 90° shifted in comparison to the other and will generate circular polarization. The paper also focused more on polarization but didn't discuss the AR beam widths of the designed antennas.

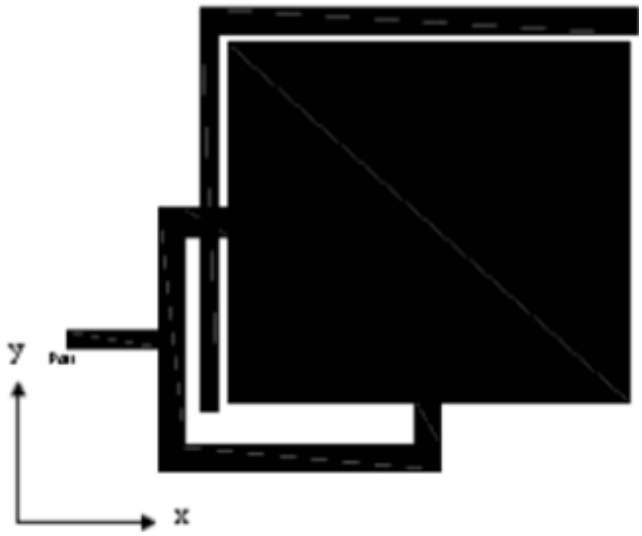

Figure 4.4 *Circularly Polarized Antenna with Dual Feed [28].*

The latest work related to the circularly polarized antenna on textile material published in 2014 uses Denim as antenna substrate [29]. Two samples of antennas were designed and circular polarization was achieved using corner truncation on the rectangular patch. The second sample includes slits on each corner to increase bandwidth. Both the antennas were fed using a probe feed along x-axis to achieve Left Hand Circular Polarization (LHCP). The main drawback of this research work is that no analysis near human body

was done to check the operability of antennas with respect to real environment. The paper also misses bending analysis and no details related to AR beam widths were mentioned.

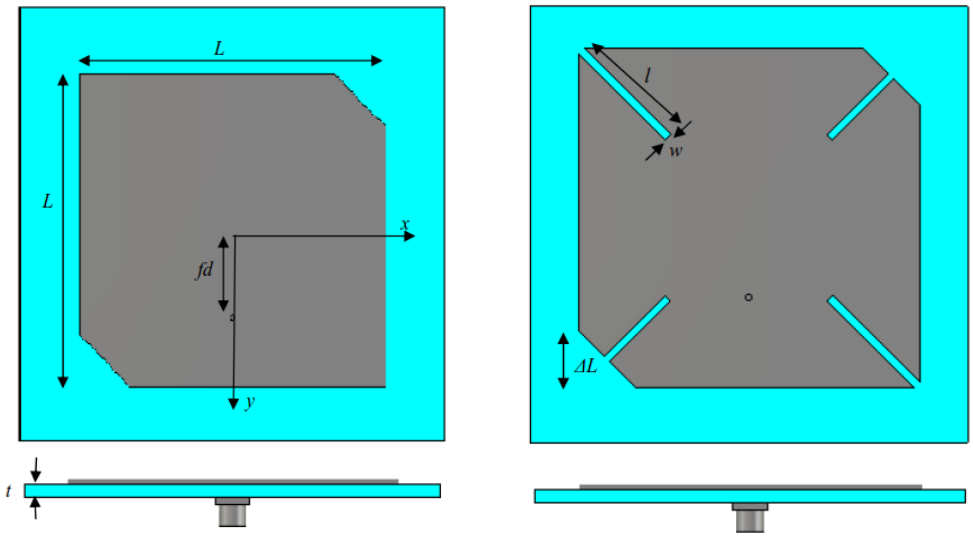

(a) (b)

Figure 4.5 *Circularly Polarized Antennas (a) Corner Truncated (b) Corner Truncated with Slits [29].*

4.4 Need of Improvement in Wearable Antennas

The literature review shows that many aspects of wearable antennas can still be improved. Following are some of these key aspects:

1. Mainly the rectangular structure of microstrip patch antennas has been used for making wearable antennas. Microstrip patch antennas have different structures like circle and triangle etc. and they can also be studied.
2. Most of the previous research missed the complete bending and near body analysis of the designed wearable antennas.
3. Rigid and fabric materials were studied more, so now new flexible substrates can be studied to design efficient wearable antennas.
4. Comparison of thin and thick substrates can be done with different bending angles to analyze the effects of bending in detail.
5. Wearable antennas can be placed on different human body parts like legs and arms so that effect of bending as well as effect of human body can be studied together.

5. CIRCULARLY POLARIZED WERABLE ANTENNA

This chapter describes the designing of circularly polarized wearable antenna on two different flexible substrates i.e. Denim and EPDM. The simulator used for the designing of the antenna is Ansoft High Frequency Structure Simulator (HFSS) 2015. HFSS uses multiple state of the art solver technologies based on finite element, integral equation or advanced hybrid methods for solving a wide range of microwave, RF and high-speed digital applications [30].

Due to the constant motion of the human body, it becomes difficult to align the polarization of the transceiver nodes for better power reception. Circular polarization (CP) operation eliminates the need to continuously align two nodes for receiving maximum power. Keeping this in mind, the antennas are designed to be circularly polarized for Industrial, Scientific and Medical (ISM) band and Wireless Body Area Network (WBAN) applications at 2.45 GHz. The reason for using two flexible substrates with different thickness is to have a good performance analysis of wearable antennas.

5.1 Design of Denim Antenna

The geometry of Denim antenna is shown in Figure 5.1. The selected Denim substrate has a thickness of 1 mm with dielectric constant (ε_r) 1.68 and loss tangent (δ) 0.03. The circular patch resonates at 2.45 GHz, while the rectangular slot "s" is used to change the path of current and generate two modes with equal amplitude and 90° phase difference for achieving circular polarization. The angle between the slot and the feed line is set to 45°. The antenna is fed by the transmission line having impedance of 50 Ω and width of 3.4 mm.

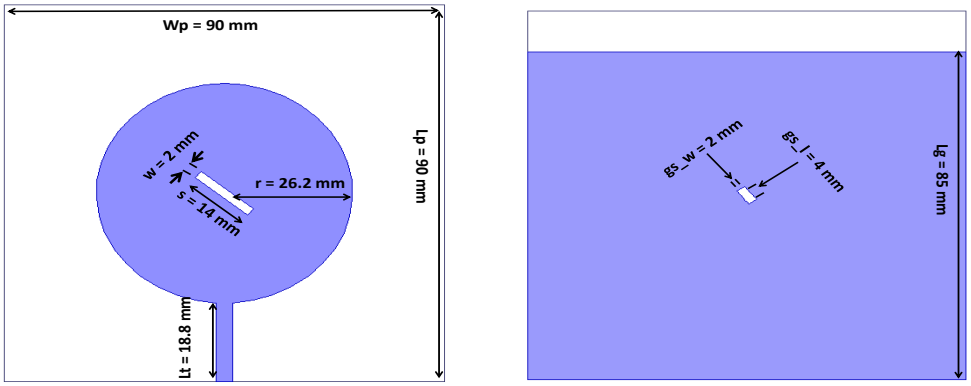

(a) (b)

Figure 5.1 *Geometry of Denim Antenna (a) Front (b) Back.*

Denim is a thin substrate which means that it will have narrow bandwidth [31]. To improve the bandwidth of the antenna partial and slotted ground plane techniques are used. The reason for this improvement in bandwidth is due to the lowering of the Q factor of the antenna, which is inversely related to the bandwidth. The Q factor of the antenna depends on the gap capacitance between the patch and the ground [31]. Using partial ground the energy stored in capacitance between the patch and the ground will be reduced which will result in the lowering of the Q factor. After partial grounding the bandwidth is increased to 80 MHz; starting from 2.40 GHz to 2.48 GHz. To cover the complete ISM band (2.40 GHz to 2.50 GHz), without changing the size of the radiating patch, slot "gs" is added to the ground plane which further lowers the Q factor of the antenna and increases the bandwidth. Due to the small size of the slot "gs", it will have very small effect on the resonant frequency. The final bandwidth of the Denim antenna, after slotted ground plane increases to 120 MHz; starting from 2.39 GHz to 2.51 GHz. The increase in backward radiation due to slot "gs" is 1.4 dB, which shows that leakage radiation from the slot is very less. The antenna uses thin substrate and has improved impedance and 3-dB AR bandwidth, in free space measured results, than the previously reported work [28][29].

5.1.1 Effect of slot "s" on Return Loss

Figure 5.2 shows the variation in return loss with parameter "s". It can be seen that increasing the length of slot "s" till certain point (14 mm), increases the return loss and shifts the frequency to lower bands, but afterwards it splits the single frequency band into two bands and starts decreasing the return loss, which is not desirable. The certain point (14 mm) is the optimal length of slot "s". The impedance bandwidth of the Denim antenna at optimal length of slot "s" is 120 MHz, starting from 2.39 GHz to 2.51 GHz, with S11 < -10 dB.

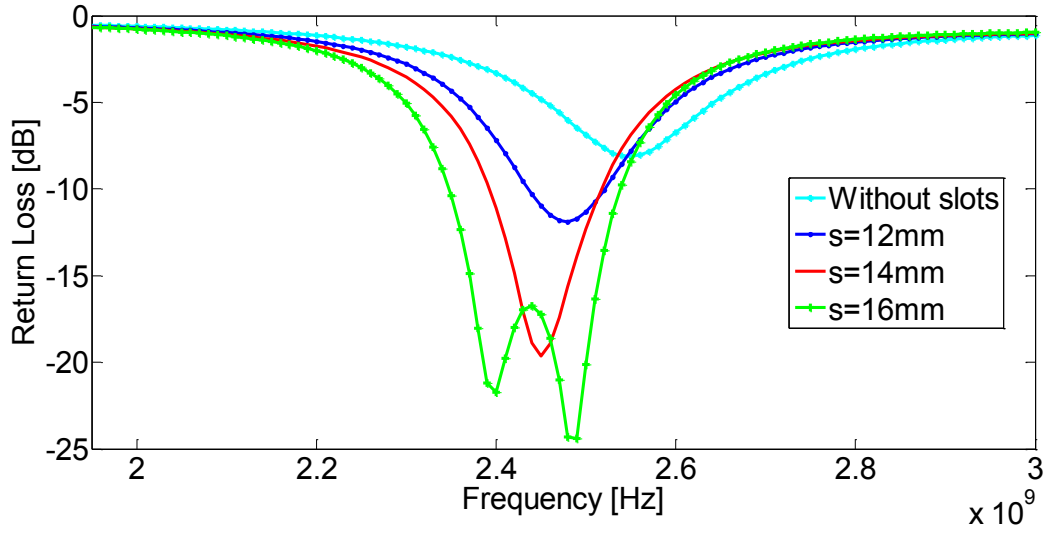

Figure 5.2 *Variation of Return Loss with slot "s".*

5.1.2 Effect of slot “s” on Axial Ratio

Figure 5.3 shows the frequency dependence of AR with different lengths of slot “s”. AR is shifted to lower frequencies by increasing the length, and the optimal length of slot “s” is 14 mm. At this length, the simulated 3-dB AR bandwidth of the antenna is 1.63 % (2.42 GHz to 2.46 GHz) or 40 MHz, which is suitable for it to achieve circular polarization at 2.45 GHz. The antenna exhibit Left Hand Circular Polarization (LHCP). The simulated 3-dB AR beam width at 2.45 GHz is approx. 86° in xz-plane (from theta -48° to +38°).

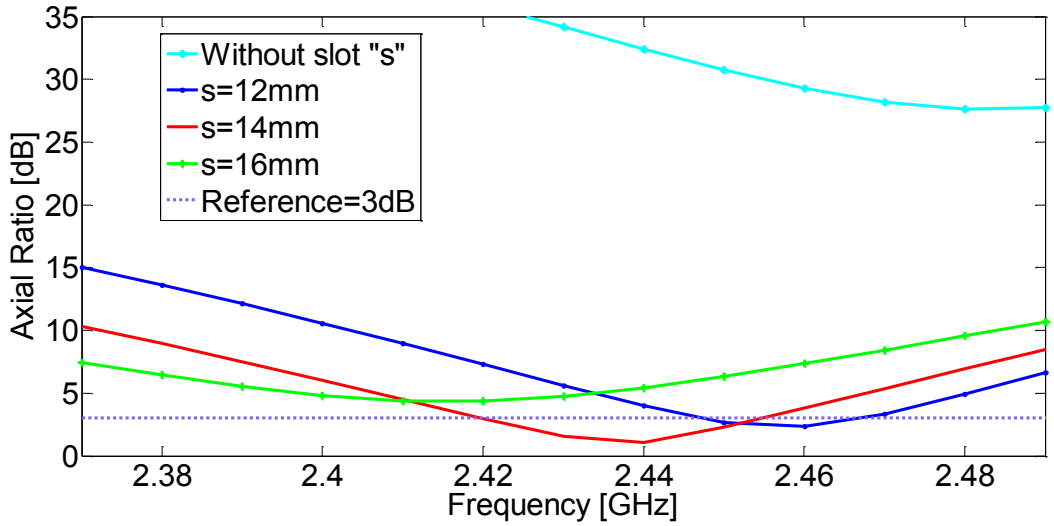

Figure 5.3 *Variation of Axial Ratio with slot “s”.*

5.1.3 3D Radiation Pattern

Figure 5.4 shows the 3D polar plot of the antenna at 2.45 GHz. The Denim antenna has a simulated gain of 2.26 dB at 2.45 GHz with the main beam directed away from the patch antenna. Due to partial grounding, a small back lobe is observed.

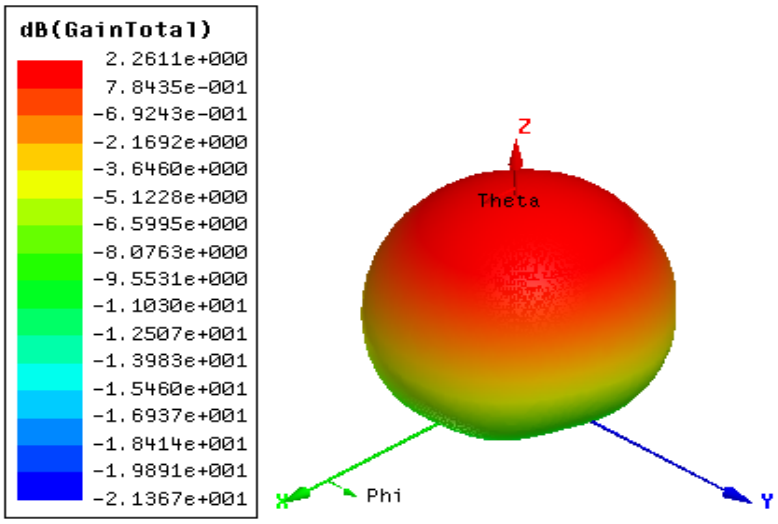

Figure 5.4 *3D Polar Plot at 2.45 GHz.*

5.1.4 Current Distribution on the Surface of Patch

Figure 5.5 shows the current distribution on the surface of the patch at 2.45 GHz with different phases. It can clearly be seen that the current rotates in a circle, which is the reason for achieving circular polarization in the antenna.

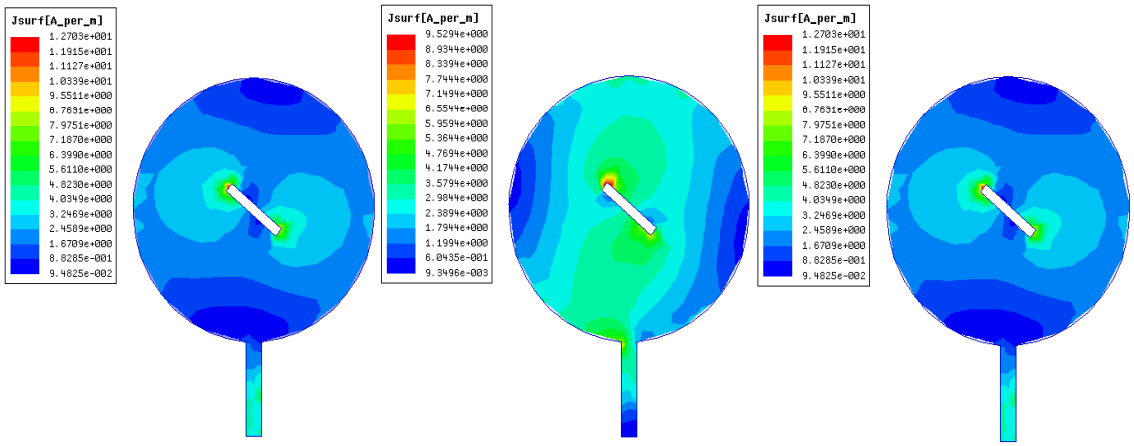

(a) (b) (c)

Figure 5.5 *Current on the Surface of Patch at 2.45 GHz (a) 0° (b) 90° (c) 180°.*

5.2 Design of EPDM Antenna

The geometry of EPDM antenna is shown in Figure 5.6. The selected EPDM foam substrate has a thickness of 3 mm with dielectric constant (ε_r) 1.23 and loss tangent (δ) 0.02. The same concept of slot "s" is used in achieving circular polarization as used in designing of Denim antenna. The angle between the slot and the feed line is set to 27°. The proposed antenna is fed by the transmission line having impedance of 50 Ω and width of 3.4 mm.

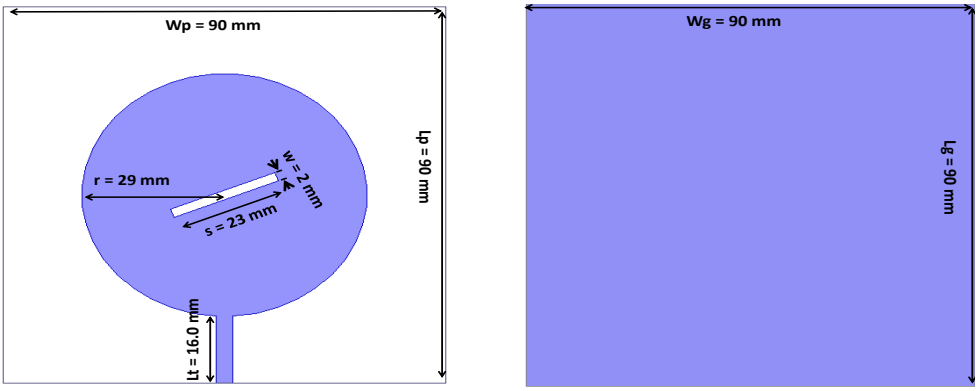

(a) (b)

Figure 5.6 *Geometry of EPDM Antenna (a) Front (b) Back.*

EPDM is thick substrate which means that it will have wide bandwidth, thus a full ground plane is used and no bandwidth improvement techniques are applied.

5.2.1 Effect of slot “s” on Return Loss

Figure 5.7 shows the variation in return loss with parameter “s”. It can be seen that increasing the length of slot “s” shifts the frequency to lower bands and improves the return loss. The length of slot “s” is set to have maximum return loss at 2.45 GHz. The optimal length of slot “s” in case of EPDM antenna is 23 mm. The impedance bandwidth of the antenna at optimal length is 150 MHz, starting from 2.3940 GHz to 2.5440 GHz, with S_{11} < -10 dB.

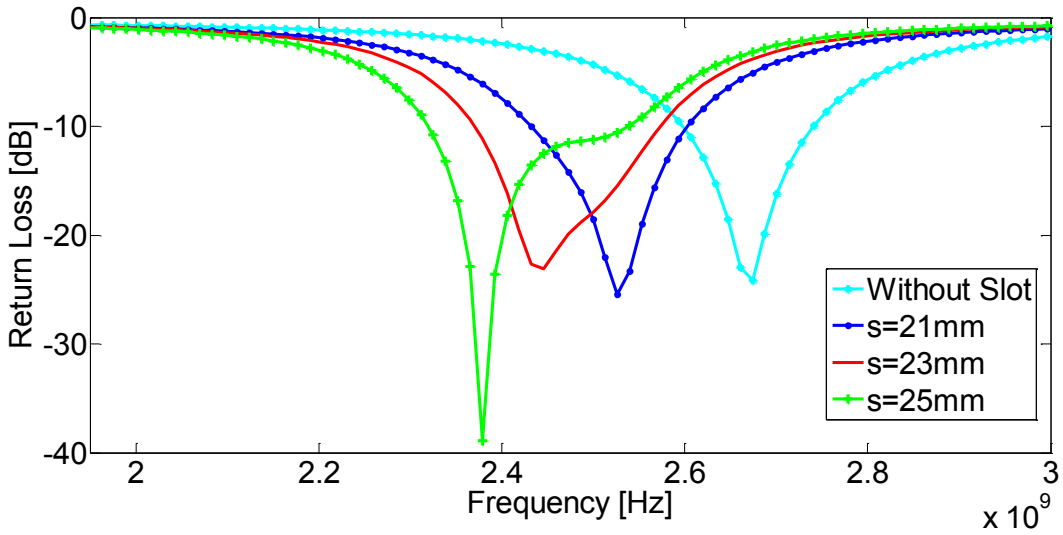

Figure 5.7 *Variation of Return Loss with slot “s”.*

5.2.2 Effect of slot “s” on Axial Ratio

Figure 5.8 shows the frequency dependence of AR with different lengths of the slot “s”. AR is shifted by changing parameter “s”, and the optimal length of slot “s” is 23 mm.

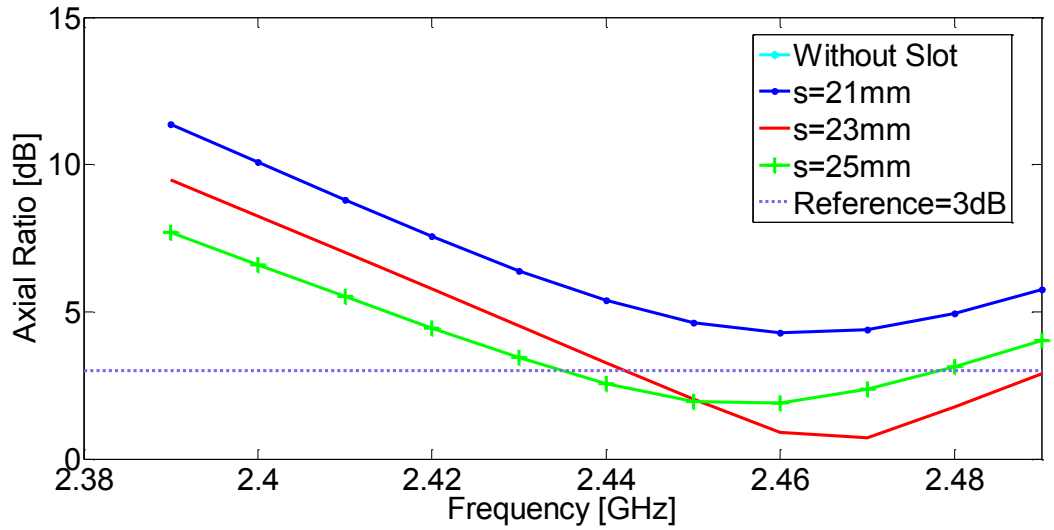

Figure 5.8 *Variation of Axial Ratio with slot “s”.*

At this length, the simulated 3-dB AR bandwidth of the antenna is 2.02 % (2.44 GHz to 2.49 GHz) or 50 MHz, which is suitable for it to achieve circular polarization at 2.45 GHz. The antenna exhibits Right Hand Circular Polarization (RHCP). The simulated 3-dB AR beam width at 2.45 GHz is approx. 104° in xz-plane (from theta -70° to +34°).

5.2.3 3D Radiation Pattern

Figure 5.9 shows the 3D polar plot of the antenna at 2.45 GHz. The EPDM antenna has a simulated gain of 6.28 dB at 2.45 GHz with the main beam directed away from the patch antenna. Due to the full ground plane, the back lobe is almost negligible.

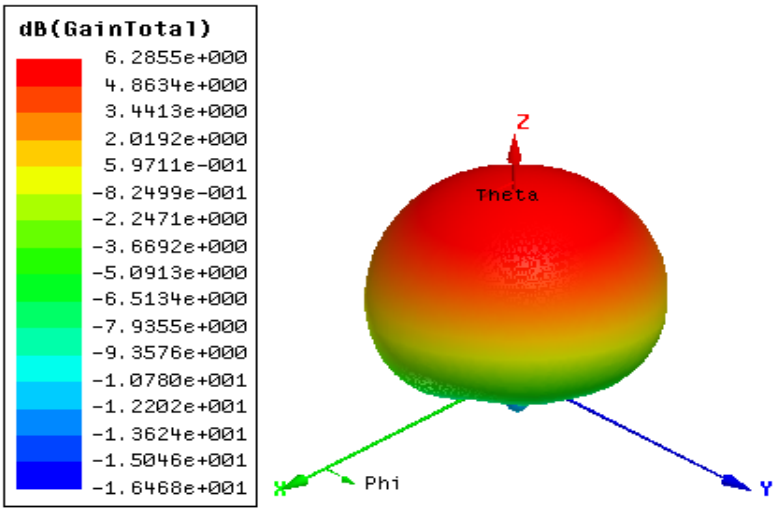

Figure 5.9 *3D Polar Plot at 2.45 GHz.*

5.2.4 Current Distribution on the Surface of Patch

Figure 5.10 shows the current distribution on the surface of the patch at 2.45 GHz with different phases. The current rotates in a circle for achieving circular polarization.

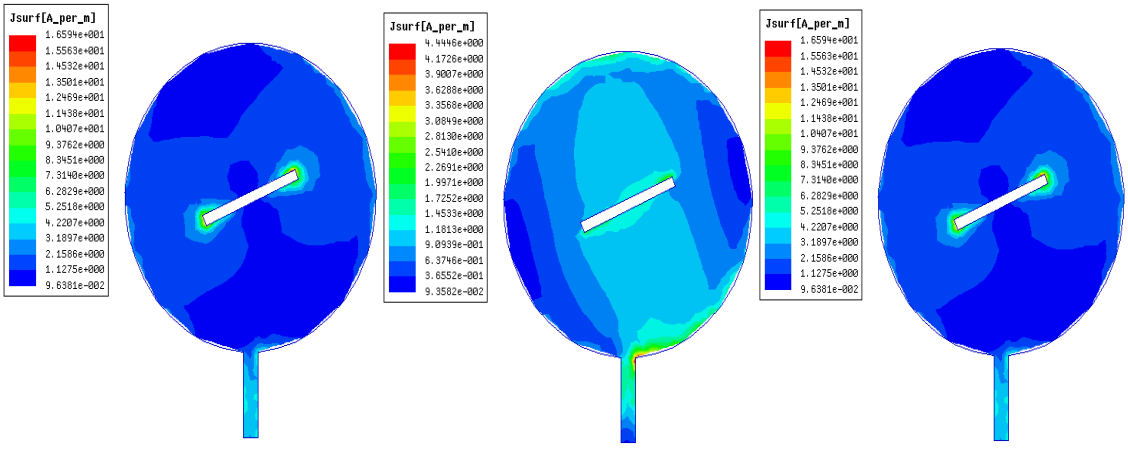

(a) (b) (c)

Figure 5.10 *Current on the Surface of Patch at 2.45 GHz (a) 0° (b) 90° (c) 180°.*

Table 5.1 compares the simulated characteristics of the designed Denim and EPDM antennas.

Table 5.1 *Comparison of Denim and EPDM Antennas.*

Characteristics	Denim	EPDM
Return Loss at 2.45 GHz	-19.62 dB	-23.10 dB
Impedance Bandwidth	120 MHz (2.39 GHz to 2.51 GHz)	150 MHz (2.39 GHz to 2.54 GHz)
Gain at 2.45 GHz	2.25 dB	6.28 dB
Radiation Efficiency at 2.45 GHz	27.50 %	66.16 %
3-dB AR bandwidth	40 MHz (2.42 GHz to 2.46 GHz)	50 MHz (2.44 GHz to 2.49 GHz)
3-dB AR beam width	86° in xz-plane (from theta -48° to +38°)	104° in xz-plane (from theta -70° to +34°)
Polarization	LHCP	RHCP

6. FREE SPACE MEASUREMENTS

This chapter discusses the free space measurement results of both Denim and EPDM antenna. Measurements are carried out using Agilent PNA E8358A Vector Network Analyzer (VNA), and near-field measurement device Satimo Starlab.

6.1 Free Space Measurements of Denim Antenna

Figure 6.1 shows the antenna during measurements in free space.

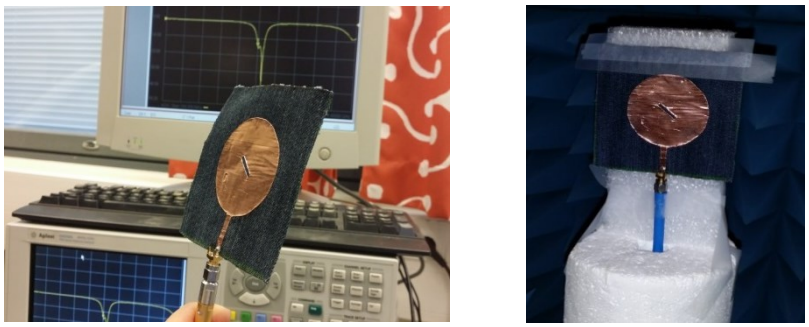

(a) (b)

Figure 6.1 *Free Space Measurement (a) VNA (b) Satimo Starlab.*

Figure 6.2 shows the comparison of simulated and measured return loss. Measured return loss is similar to the simulated one with a shift towards higher frequencies. The reason for shifting is inaccuracies in the fabrication as the antenna is fabricated by manually cutting the jeans and copper tape. The measured impedance bandwidth of the antenna is 160 MHz (2.42 GHz – 2.58 GHz).

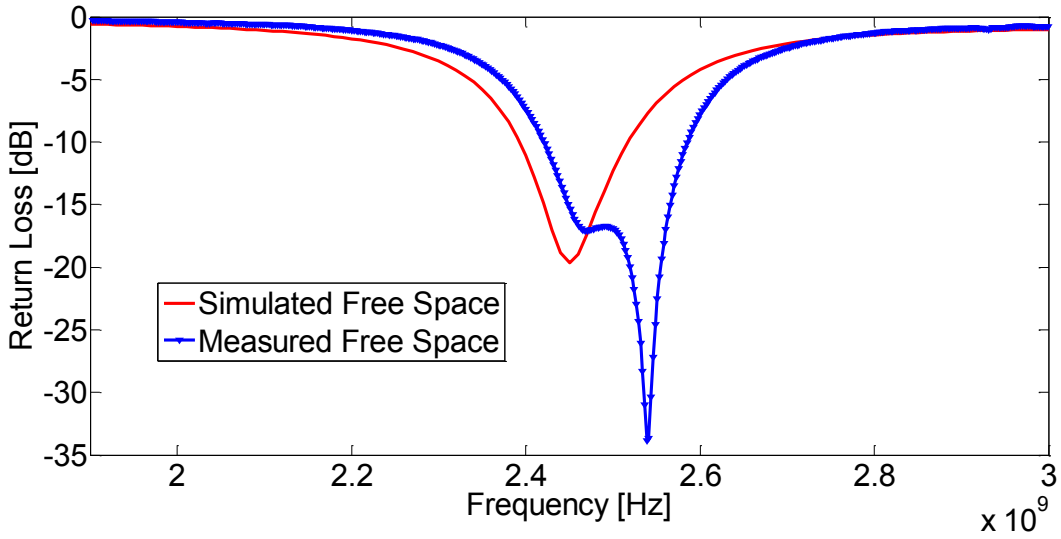

Figure 6.2 *Simulated and Measured Free Space Return Loss.*

The same trend is followed in AR, as it shifts toward higher frequencies with circular polarization (AR < 3dB). Figure 6.3 shows the comparison of simulated and measured AR. The measured 3-dB AR bandwidth of the antenna is 60 MHz (2.45 GHz – 2.51 GHz).

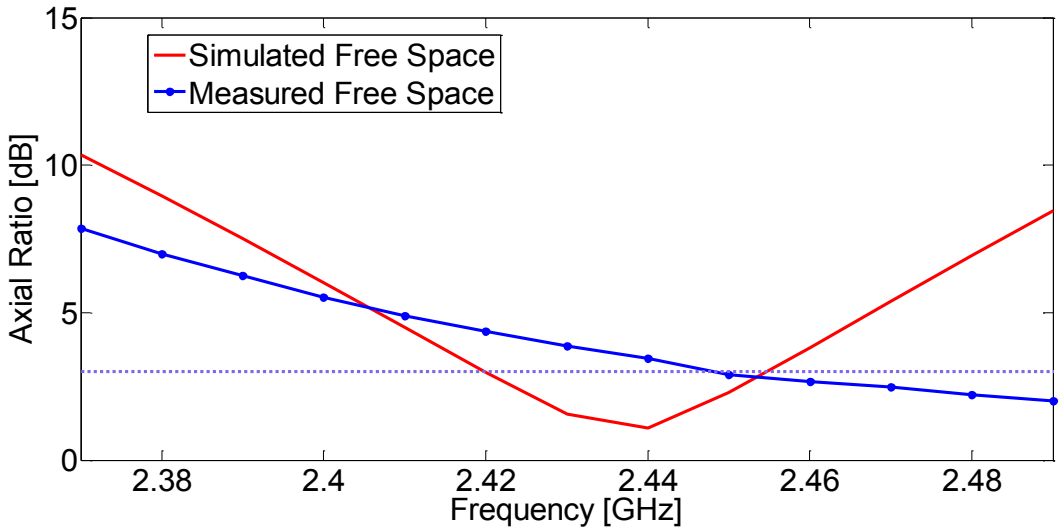

Figure 6.3 *Simulated and Measured Free Space Axial Ratio.*

Figure 6.4 shows the comparison of simulated and measured results in terms of the AR and gain at 2.45 GHz in xz-plane. The measured 3-dB AR beam width at 2.45 GHz is approx. 218° in xz-plane (from -157° to +61°). Free space antenna measurements show that the antenna can efficiently operate on the desired frequency band with circular polarization in the main beam. The measured Front to Back Ratio (FBR) is 20.09 dB which is good for wearable applications as maximum radiation is directed away from the antenna even with partial grounding.

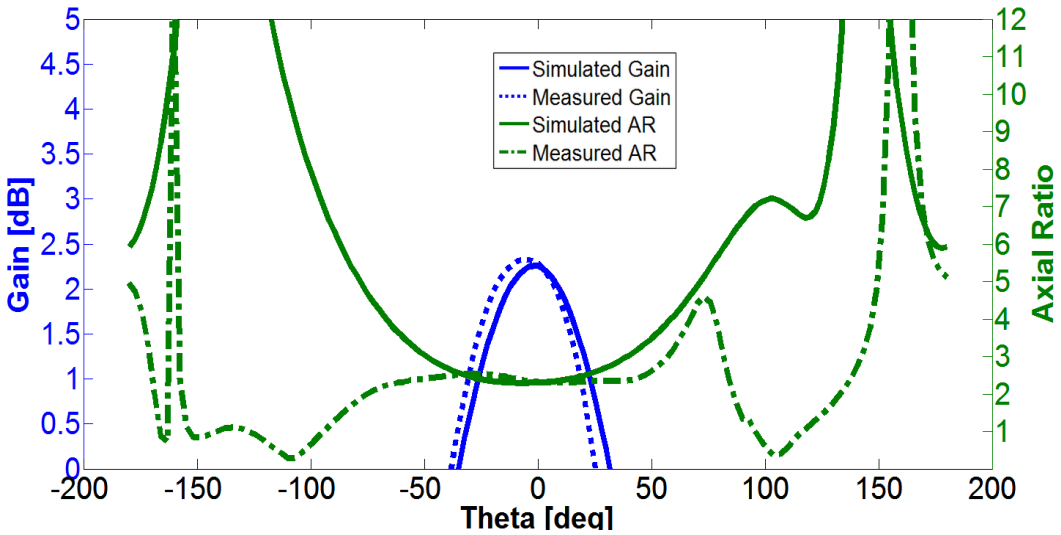

Figure 6.4 *Simulated and Measured Results for Gain and Axial Ratio at 2.45 GHz.*

Figure 6.5 shows the comparison of simulated and measured antenna efficiency. The antenna has around 25 % efficiency at 2.45 GHz.

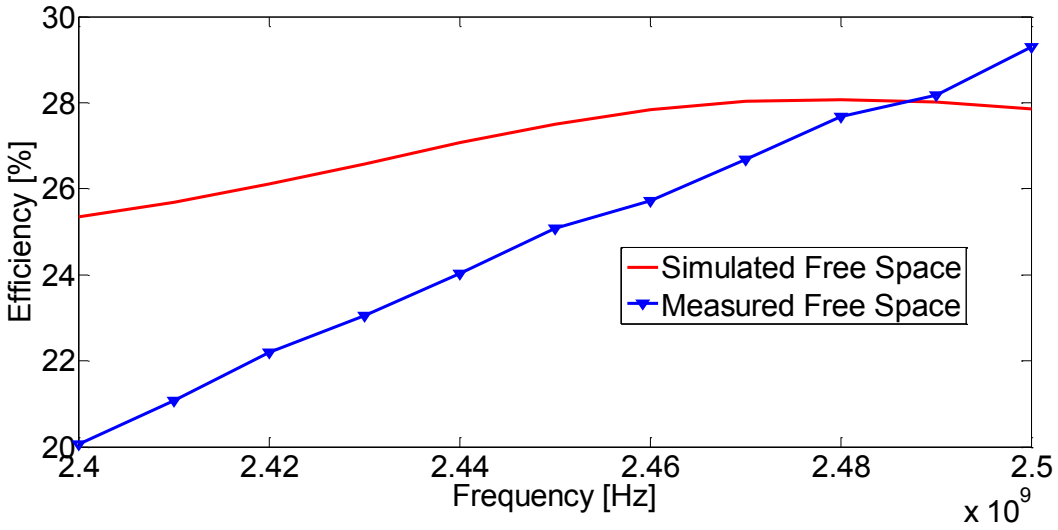

Figure 6.5 *Simulated and Measured Efficiency.*

6.1.1 Bending Analysis of Denim Antenna

To demonstrate the effect of bending, two cylindrical shaped plastic bottles with radii 50 mm (small cylinder) and 75 mm (large cylinder) are used. Greater the radius of the cylinder, smaller the bending angle, and vice versa. The selected radii are for typical human body parts like arms and legs etc. The material of the cylinder is selected so that it does not affect the surface currents of the antenna. The antenna is bent on the cylinder in both xz-plane and yz-plane. Transparent paper tape is used to hold the antenna in the proper place during measurements. Performance of the antenna in bending is evaluated by analyzing the effects on return loss, axial ratio and radiation characteristics. Radiation characteristics include radiation patterns (xz-plane and yz-plane), gain, and radiation efficiency at 2.45 GHz. Figure 6.6 shows the bent antenna in different planes.

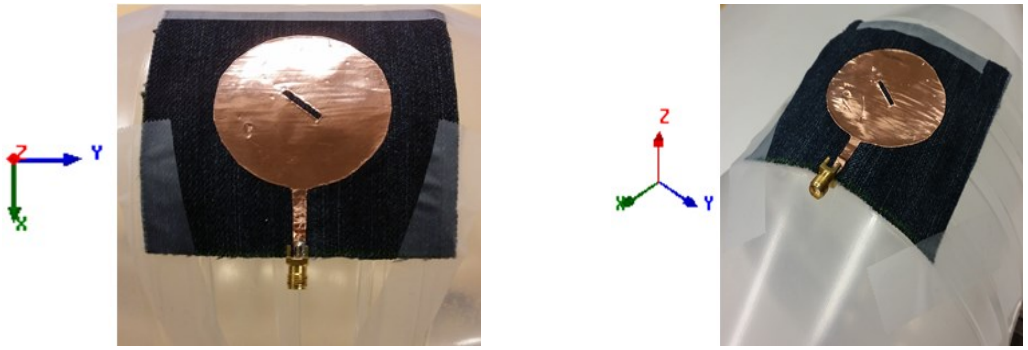

(a) (b)

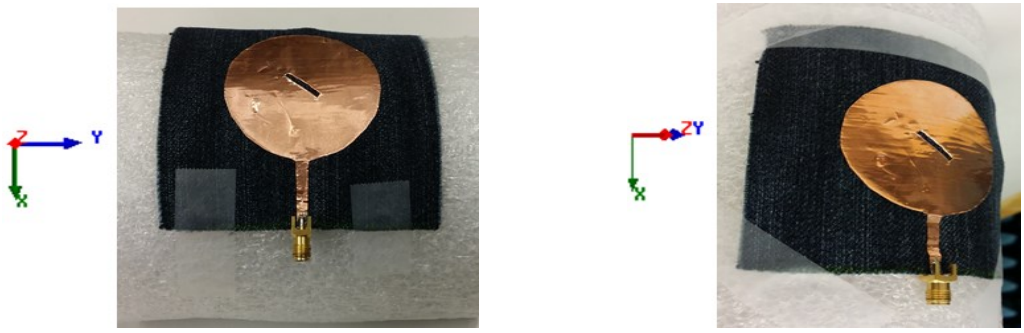

(c) (d)

Figure 6.6 *Bending (a) xz 75mm (b) yz 75mm (c) xz 50mm (d) yz 50mm.*

Figure 6.7 compares the measured return loss of the antenna in flat and bent states. In general, bending an antenna changes the effective length which ultimately changes the resonant frequency. Increasing the bending, decreases the effective length, thus the resonant frequency is shifted to higher bands. From the measured data, this is very clear in case of bending on the small cylinder. Return loss on the large cylinder is almost similar to the measured return loss of the flat antenna because of the small bending angle. The impedance band breaks into two when the antenna is bent in xz-plane on the large cylinder. Effect of bending in yz-plane is the worst as it shifts the resonant frequency to higher bands as well as degrades the return loss. One reason for this can be that the effective dimensions of transmission line and slot "s" are slightly modified, which detunes the input matching of the antenna. Compared with the measured results (flat antenna), yz-plane bending does not have significant effect on the return loss at 2.45 GHz. In all studied cases of the antenna bending, except small cylinder in yz-plane, the measured impedance bandwidth is larger (25 % to 50 %) than the simulated impedance bandwidth of 120 MHz.

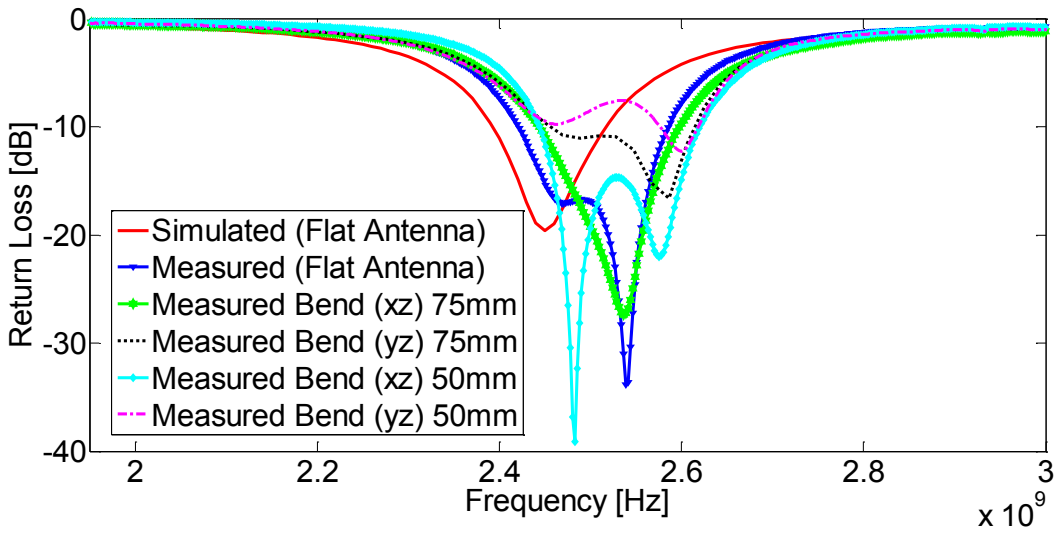

Figure 6.7 *Variation of Return Loss with Bending.*

Table 6.1 summarizes the change in return loss and bandwidth of the antenna with bending.

Table 6.1 *Change in Return Loss and Bandwidth of the Antenna with Bending.*

Antenna Position	Return Loss at 2.45 GHz [dB]	Bandwidth [MHz]
Simulated (Flat)	-19.620	120 (2.39 GHz – 2.51 GHz)
Measured (Flat)	-15.378	160 (2.42 GHz – 2.58 GHz)
Bending 50 mm *xz*	-11.850	180 (2.44 GHz – 2.62 GHz)
Bending 50 mm *yz*	-9.537	50 (2.57 GHz – 2.62 GHz)
Bending 75 mm *xz*	-11.010	150 (2.44 GHz – 2.59 GHz)
Bending 75 mm *yz*	-9.628	160 (2.45 GHz – 2.61 GHz)

Figure 6.8 compares the measured AR of the antenna in flat and bent states. The measured AR follows the same trend as measured return loss in different bending scenarios. AR < 3 dB is maintained at 2.45 GHz when the antenna is bent in xz-plane, while in yz-plane, AR degrades at 2.45 GHz. Circular polarization changes to linear (or is highly elliptical) in yz-plane bending. Improvement in AR is observed for xz-plane bending. Circular polarization can easily change with bending because both length and width are in resonance with 90° phase shift and bending affects the effective resonating area of the patch. It is always preferred to place the textile antenna on flat body parts like back and chest etc. One solution to this problem can be designing an elliptically polarized antenna and bending it along the longer dimension to achieve circular polarization. The antenna then should be placed in specific bending for use in the wearable applications.

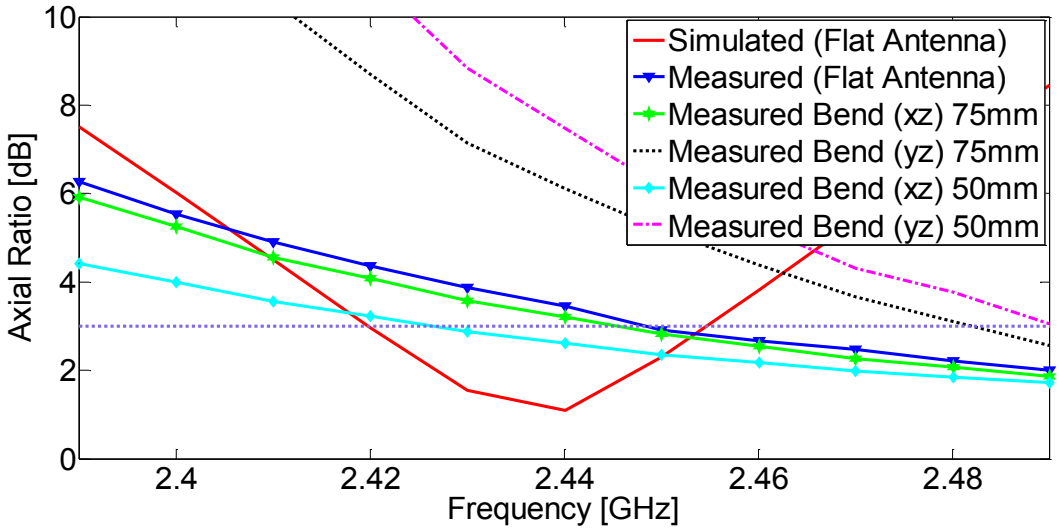

Figure 6.8 *Variation of Axial Ratio with Bending.*

Figure 6.9 shows the 2D radiation patterns of the antenna in xz-plane and yz-plane. Position of the antenna is also shown in Figure 6.9 to have a better understanding about the radiation pattern around it. In xz-plane bending, the beam width increases in both planes (xz and yz) on the larger cylinder, but as the bending is increased more by placing the antenna on the smaller cylinder, the beam width tends to increase more in the plane of bending. The same change is observed in yz-plane bending. This leads to the conclusion

that antenna bending broadens the radiation pattern in the bending plane. The gain and the efficiency of the antenna mainly reduce with bending.

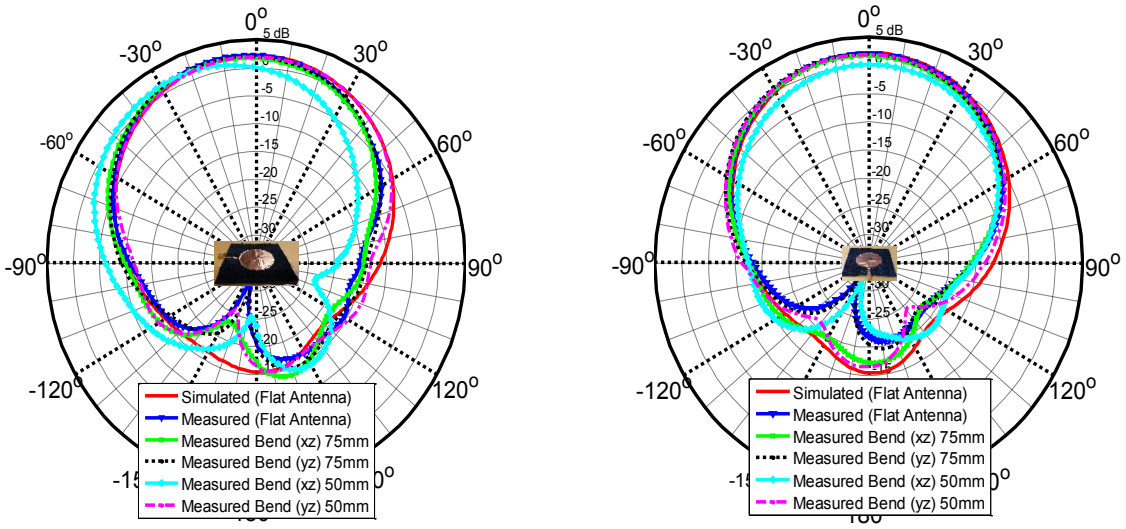

(a) (b)

Figure 6.9 *Radiation Patterns. (a) xz-plane. (b) yz-plane.*

Table 6.2 summarizes the changes in radiation characteristics of the antenna with bending. The measured results follow the theoretical relationship between gain, efficiency and directivity the antenna given in equation (3.7).

Table 6.2 *Changes in Radiation Characteristics of the Antenna with Bending.*

Antenna Position	3 dB Beam width (xz-plane or Phi 0°)	3 dB Beam width (yz-plane or Phi 90°)	Peak Gain at 2.45 GHz [dB]	Efficiency at 2.45 GHz [%]
Simulated (Flat)	77° (+37° to -40°)	72° (+37° to -35°)	2.2612	27.505
Measured (Flat)	73° (+30° to -43°)	74° (+35° to -39°)	2.2524	25.076
Bending 50 mm *xz*	78° (+13° to -65°)	74° (+37° to -37°)	1.6579	22.387
Bending 50 mm *yz*	74° (+32° to -42°)	80° (+37° to -43°)	1.9904	26.699
Bending 75 mm *xz*	78° (+30° to -48°)	75° (+32° to -43°)	1.8872	24.582
Bending 75 mm *yz*	77° (+31° to -46°)	77° (+33° to -44°)	2.1133	26.345

6.2 Free Space Measurements of EPDM Antenna

The second antenna is fabricated on EPDM foam substrate. It has light weight, excellent shock resistance, high flexibility and can be attached to any curved surface [32]. The important property of being light weight makes it comfortable to wear as a substrate for BAN or wearable applications. The dielectric constant of EPDM is almost constant in a wide temperature range from −40˚C to +120˚C which means that dielectric properties of

the material will not change if used in extreme environments, for example freezing cold or hot weather [32]. Figure 6.10 shows the environmental adaptability of EPDM foam in free space and near the human arm.

(a) (b)

Figure 6.10 *Environmental Adaptability of EPDM foam (a) In free space (b) On hand.*

According to [32][33][34], rubber based substrate can naturally and forcibly retract to its original dimensions after deformation. Figure 6.11 shows the antenna during measurements in free space.

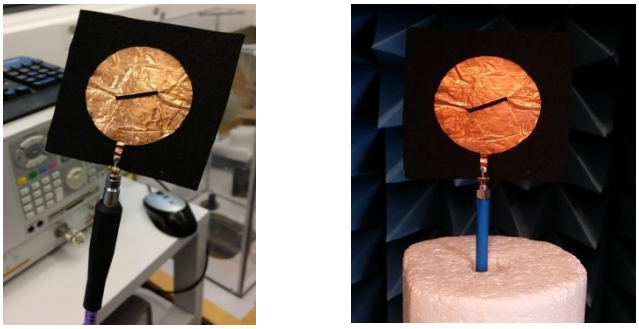

(a) (b)

Figure 6.11 *Free Space Measurement (a) VNA (b) Satimo Starlab.*

Figure 6.12 compares the simulated and measured return loss of the antenna in the flat position. It can be seen that the return loss is shifted to lower frequencies. One reason for this shift can be the inaccuracies introduced due to manual fabrication. The measured impedance bandwidth of the antenna is 120 MHz, starting from 2.36 GHz to 2.48 GHz, with $S_{11} < -10$ dB.

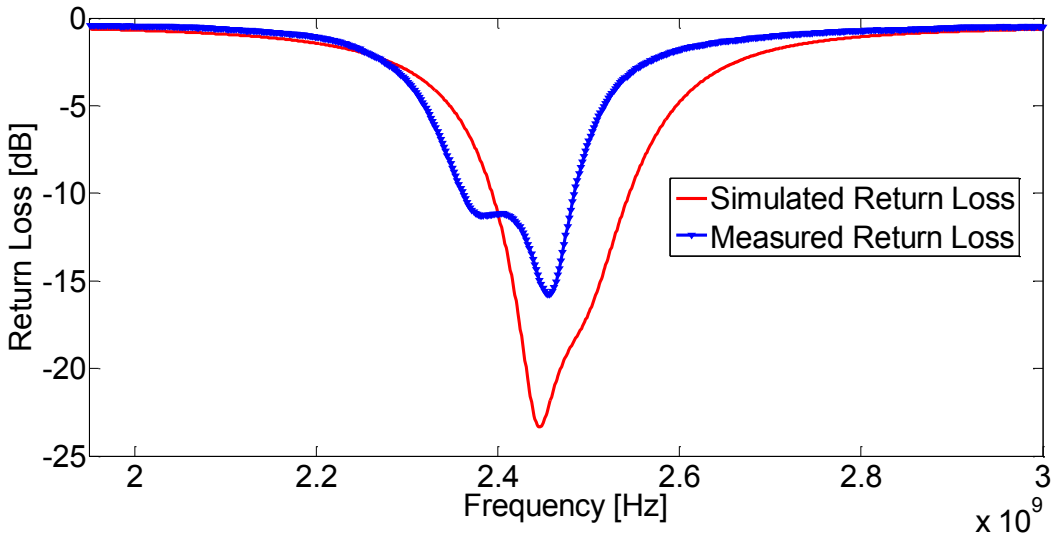

Figure 6.12 *Simulated and Measured Free Space Return Loss.*

Figure 6.13 shows the comparison of simulated and measured axial ratio. The results show that measured AR < 3 dB for the whole ISM band.

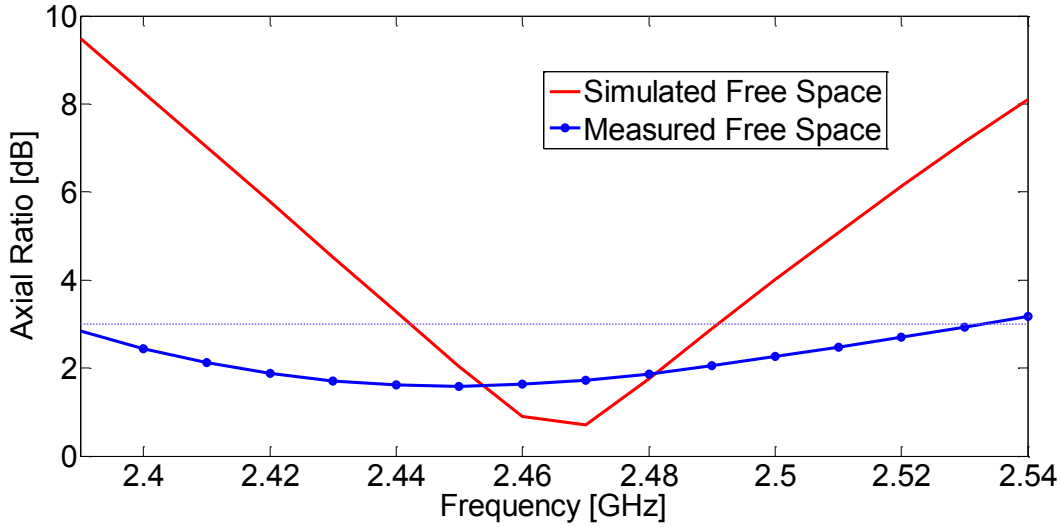

Figure 6.13 *Simulated and Measured Free Space Axial Ratio.*

Figure 6.14 shows the comparison of simulated and measured results in terms of the AR and gain at 2.45 GHz in yz-plane. The measured 3-dB AR beam width at 2.45 GHz is approx. 130° in yz-plane (From theta -85° to +45°). The measured 3-dB AR bandwidth is 3.66 % (2.41 GHz to 2.50 GHz) or 90 MHz. The measured gain of the fabricated antenna at 2.45 GHz is 6.03 dB. The measured efficiency of the antenna in the operating band is approx. 62 % – 63 %.

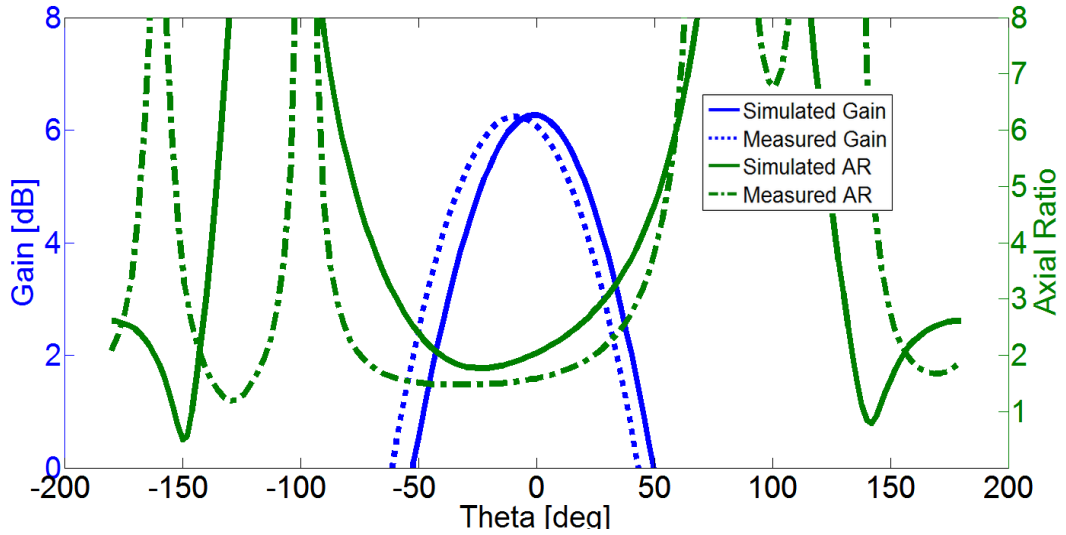

Figure 6.14 *Simulated and Measured Results for Gain and Axial Ratio at 2.45 GHz.*

Figure 6.15 shows the comparison of simulated and measured antenna efficiency. The antenna has around 63 % efficiency at 2.45 GHz.

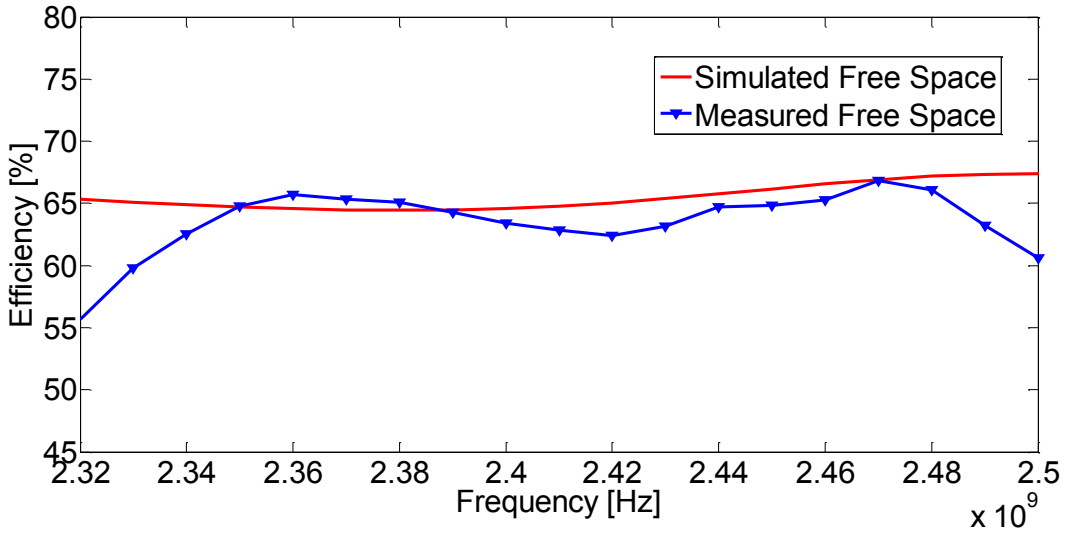

Figure 6.15 *Simulated and Measured Efficiency.*

6.2.1 Bending Analysis of EPDM Antenna

The same method for the bending analysis of EPDM antenna is used as it was in case of Denim antenna. Figure 6.16 shows the bent antenna in different planes.

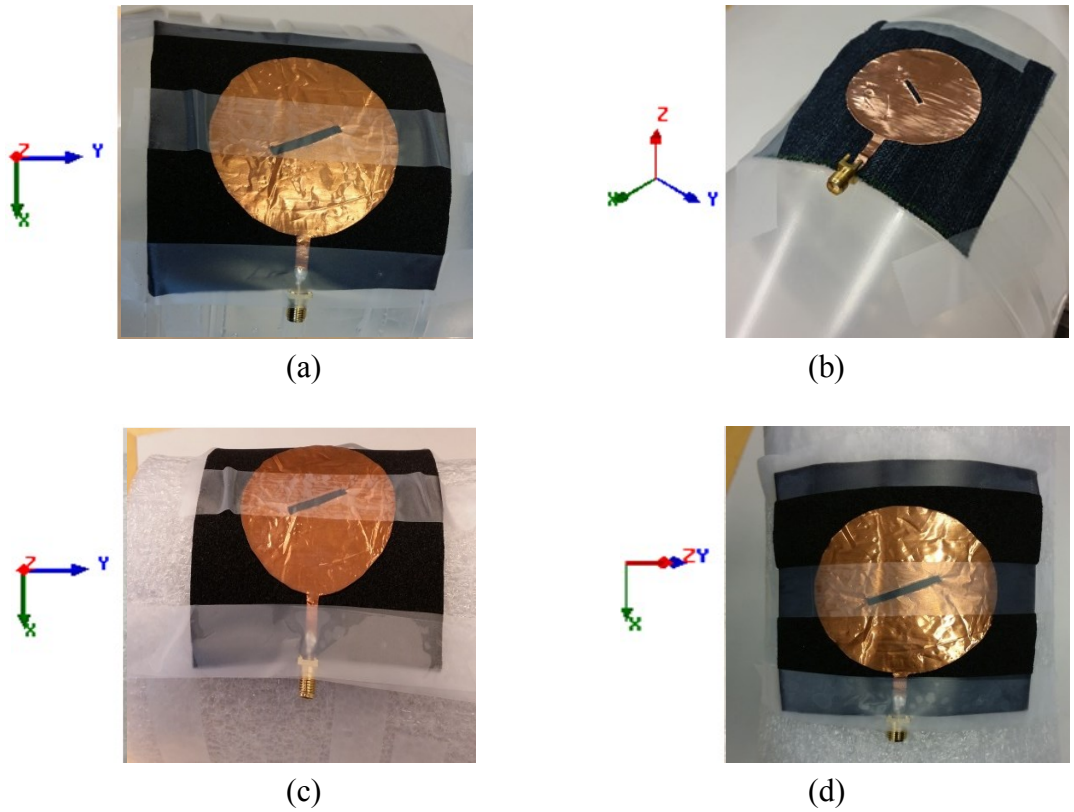

(a) (b)

(c) (d)

Figure 6.16 *Bending (a) xz 75mm (b) yz 75mm (c) xz 50mm (d) yz 50mm.*

Figure 6.17 compares the measured return loss of the antenna in flat and bent states. In general, bending an antenna changes the effective length which ultimately changes the resonant frequency. Increasing the bending, decreases the effective length, thus the resonant frequency is shifted to higher bands. From the measured data, it is seen that return loss is improved on higher frequency bands. Return loss is almost similar to the measured return loss of the flat antenna. Compared with the measured results (flat antenna), bending does not have significant effect on the return loss of EPDM antenna at 2.45 GHz. In all the studied cases of the antenna bending, the measured impedance bandwidth is larger (10 % to 15 %) than the simulated impedance bandwidth of 150 MHz.

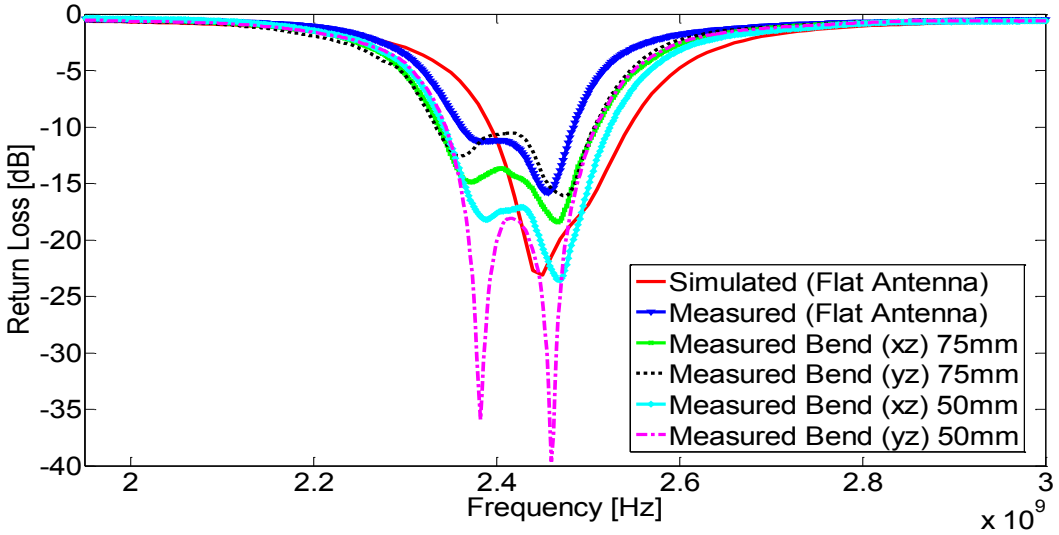

Figure 6.17 *Variation of Return Loss with Bending.*

Table 6.3 summarizes the change in return loss and bandwidth of the antenna with bending.

Table 6.3 *Change in Return Loss and Bandwidth of the Antenna with Bending.*

Antenna Position	Return Loss at 2.45 GHz [dB]	Bandwidth [MHz]
Simulated (Flat)	-23.10	150 (2.39 GHz – 2.54 GHz)
Measured (Flat)	-15.43	120 (2.36 GHz – 2.48 GHz)
Bending 50 mm *xz*	-20.41	180 (2.34 GHz – 2.52 GHz)
Bending 50 mm *yz*	-24.80	160 (2.34 GHz – 2.50 GHz)
Bending 75 mm *xz*	-16.91	170 (2.33 GHz – 2.50 GHz)
Bending 75 mm *yz*	-14.06	170 (2.33 GHz – 2.50 GHz)

Figure 6.18 compares the measured AR of the antenna in flat and bent states. The measured AR follows the same trend as the measured return loss in different bending scenarios. AR < 3dB is maintained at 2.45 GHz for all the bending cases.

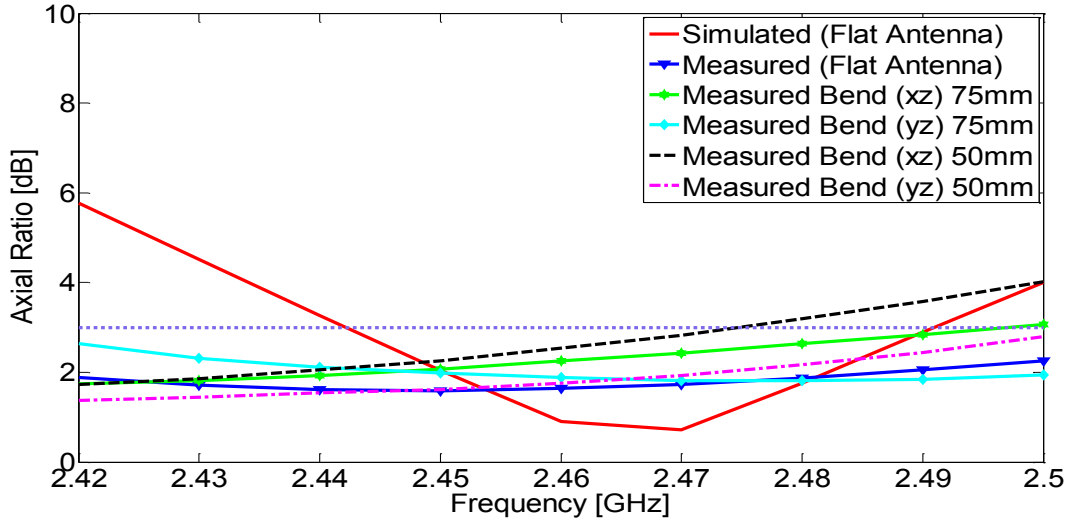

Figure 6.18 *Variation of Axial Ratio with Bending.*

Figure 6.19 shows the 2D radiation patterns of the antenna in xz-plane and yz-plane. The same trend is seen in bent radiation patterns as the radiation pattern broadens.

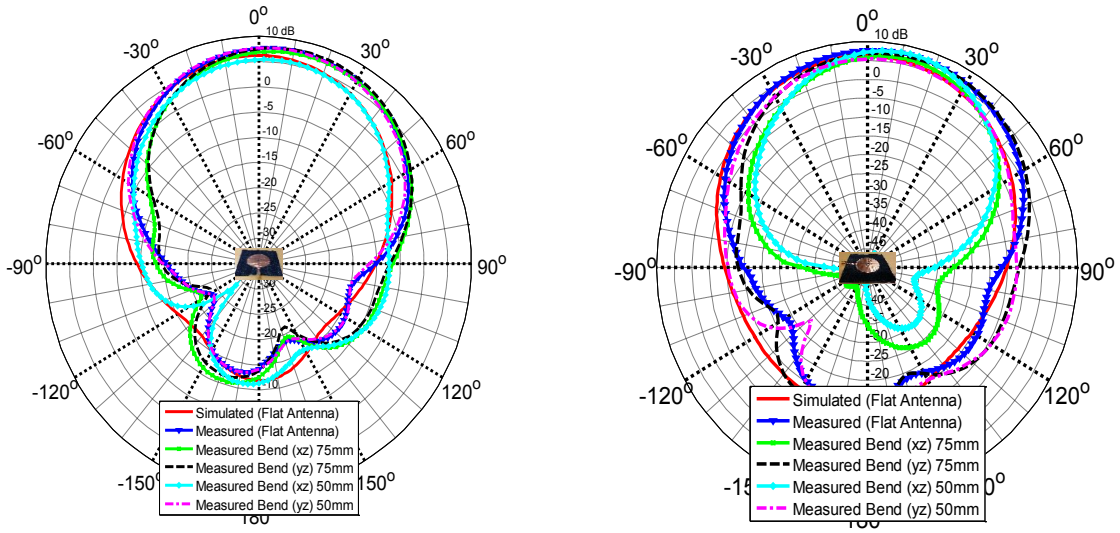

(a) (b)

Figure 6.19 *Radiation Patterns (a) xz-plane. (b) yz-plane.*

Table 6.4 summarizes the changes in radiation characteristics of the antenna with bending.

Table 6.4 *Changes in Radiation Characteristics of the Antenna with Bending.*

Antenna Position	3 dB Beam width (xz-plane or Phi 0°)	3 dB Beam width (yz-plane or Phi 90°)	Peak Gain at 2.45 GHz [dB]	Efficiency at 2.45 GHz [%]
Simulated (Flat)	68° (+31° to -37°)	71° (+35° to -36°)	6.2840	66.168
Measured (Flat)	68° (+33° to -35°)	72° (+34° to -38°)	6.0300	62.000
Bending 50 mm *xz*	70° (+33° to -37°)	78° (+41° to -37°)	5.9845	59.332
Bending 50 mm *yz*	71° (+36° to -35°)	67° (+34° to -33°)	6.0197	58.729
Bending 75 mm *xz*	70° (+33° to -37°)	78° (+37° to -41°)	6.1269	62.618
Bending 75 mm *yz*	72° (+36° to -36°)	68° (+36° to -32°)	6.3154	65.715

7. ON-BODY MEASUREMENTS

This chapter describes the importance of on-body measurements of wearable antennas. The first part of this chapter explains the properties of human body and its effects on a nearby antenna. The later part analyses the effects of human body on both of the designed antennas.

7.1 Properties of Human Body

The real time applications of the wearable antenna operate near human body vicinity. Water constitutes two-thirds of human body and it is attributed as polar in nature, the antenna property changes in the vicinity of human body due to the polarization of water molecules in the presence of electromagnetic radiations. This phenomenon is known as dielectric loading. The electrical properties of human body change with frequency. Table 7.1 tabulates the properties of different human body layers at 2.45 GHz [35].

Table 7.1 *Properties of Human Body at 2.45 GHz [35].*

Tissue	Conductivity [S/m]	Relative Permittivity	Loss tangent	Wavelength [m]	Penetration depth [m]
Dry Skin	1.464	38.007	0.28262	0.019657	0.022573
Wet Skin	1.19	42.853	0.27255	0.018524	0.022029
Fat	0.10452	5.01	0.14524	0.053113	0.11702
Muscle	1.88	52.729	0.24194	0.016731	0.02233
Nerve	1.0886	30.145	0.26494	0.022097	0.027006
Blood	2.48	58.264	0.32046	0.015834	0.016122

All the commonly used antenna parameters, such as resonant frequency, bandwidth, radiation pattern, and particularly efficiency are likely to change radically as an antenna moves closer to the body and therefore a free space design may only be a rough approximation of antenna suitability.

7.2 Need of On-body Measurements

In WBAN applications, single or multiple antennas are mounted as transceiver nodes on human body. The transceiver nodes may communicate with one another or some remote server for sending data depending on the application. The problem arises when the antenna is placed on human body as not all parts of the human body are flat. Performance of antennas designed to operate on the bent body parts like arm and leg, should be checked in real time environment.

7.3 On-body Measurements of Denim Antenna

To have a better understanding, bending of the Denim antenna is done in both xz-plane and yz-plane on leg and arm of a male.

7.3.1 Bending of Denim Antenna in xz-plane

Figure 7.1 shows the antenna's position during bending measurements in xz-plane.

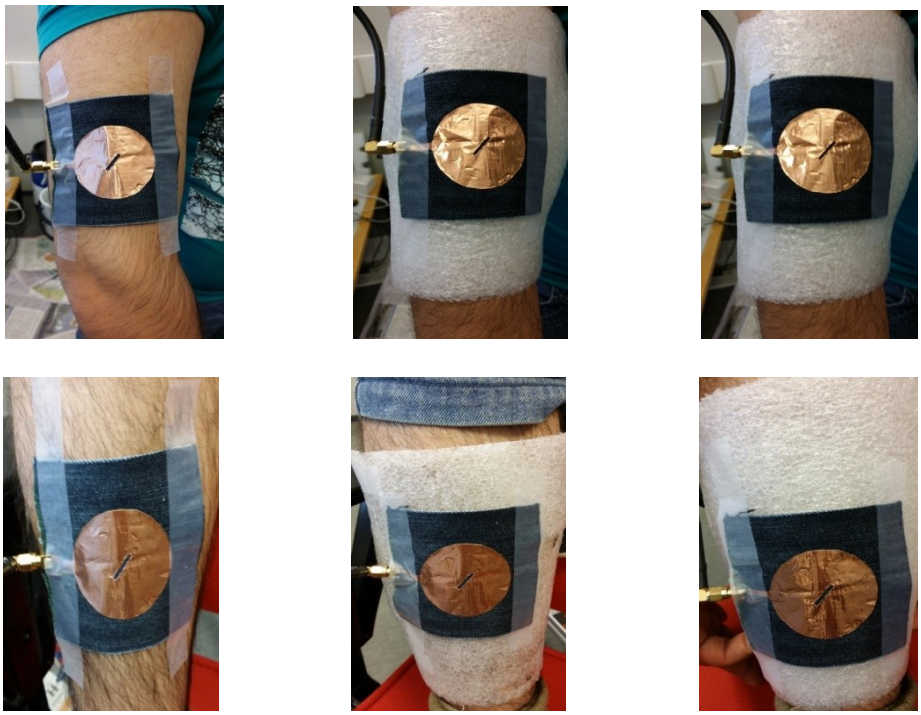

Figure 7.1 *Bending of Denim Antenna in xz-plane*

Figure 7.2 and Figure 7.3 show the variation of return loss on the arm and the leg in bending condition along the xz-plane. The near body results show larger bandwidth, when the antenna is directly attached to the skin, compared with the measured free space results. This increase in bandwidth is due to the lowering of the Q factor of the antenna near human body. The return loss has significantly decreased but the antenna still operates on 2.45 GHz in all cases of bending in xz-plane.

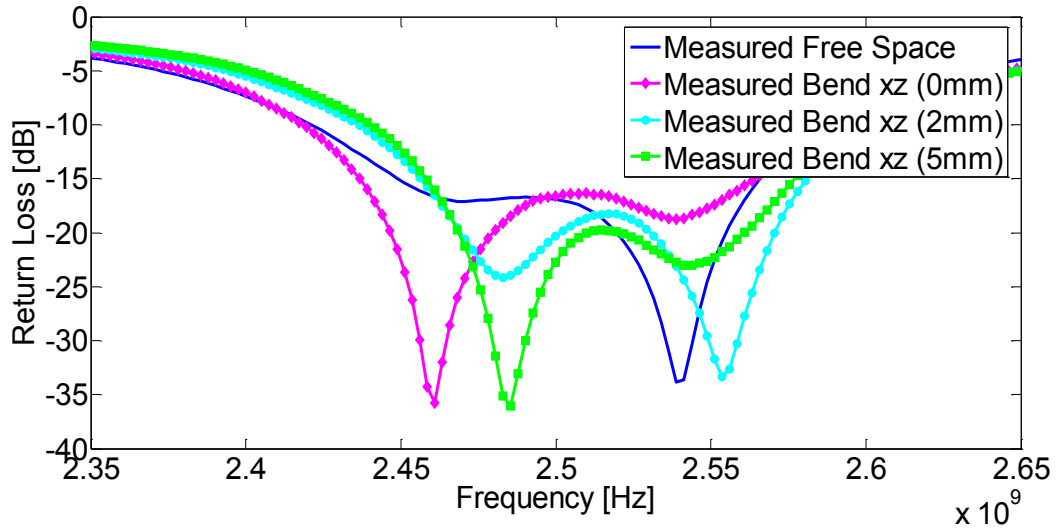

Figure 7.2 *Variation in Return Loss with Bending in xz-plane on the Arm.*

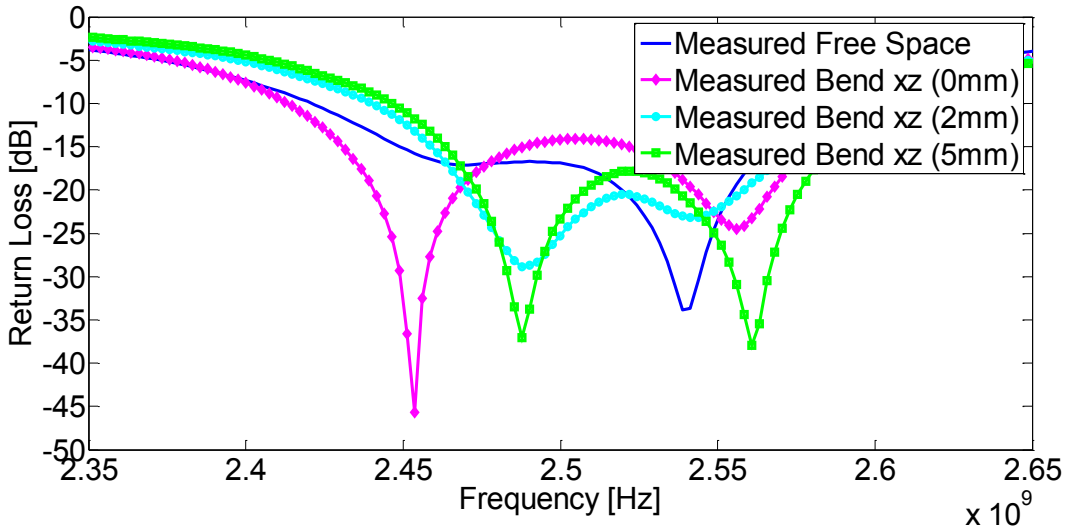

Figure 7.3 *Variation in Return Loss with Bending in xz-plane on the Leg.*

Table 7.2 tabulates the variation in return loss for different bending conditions along the xz-plane with -10 dB criteria of return loss.

Table 7.2 *Return Loss and Impedance Bandwidth for Bending in xz-plane.*

Antenna Position		Return Loss at 2.45 GHz	Bandwidth [MHz] (-10 dB criteria)
Arm	0 mm	-21.55	171 (2.420 – 2.591)
	2 mm	-12.75	154 (2.437 – 2.591)
	5 mm	-11.94	156 (2.442 – 2.598)
Leg	0 mm	-29.32	186 (2.415 – 2.601)
	2 mm	-11.84	156 (2.442 – 2.598)
	5 mm	-10.53	159 (2.447 – 2.606)

7.3.2 Bending of Denim Antenna in yz-plane

Figure 7.4 shows the antennas position during bending measurements in yz-plane.

Figure 7.4 *Bending of Denim Antenna in yz-plane.*

Figure 7.5 and Figure 7.6 show the variation of return loss on the arm and the leg in in bending condition along the yz-plane. The near body results show that in bending condition along the yz-plane, the resonant frequency shifts to higher bands as well as the return loss degrades. One reason for this can be that the effective dimensions of transmission line and the slot "s" are slightly modified, which detunes the input matching of the antenna. The measured near body results show larger bandwidth compared with the measured free space results which is also seen in the bending conditions along the xz-plane. The return loss has significantly decreased but the antenna still operates on 2.45 GHz in all cases of bending in yz-plane.

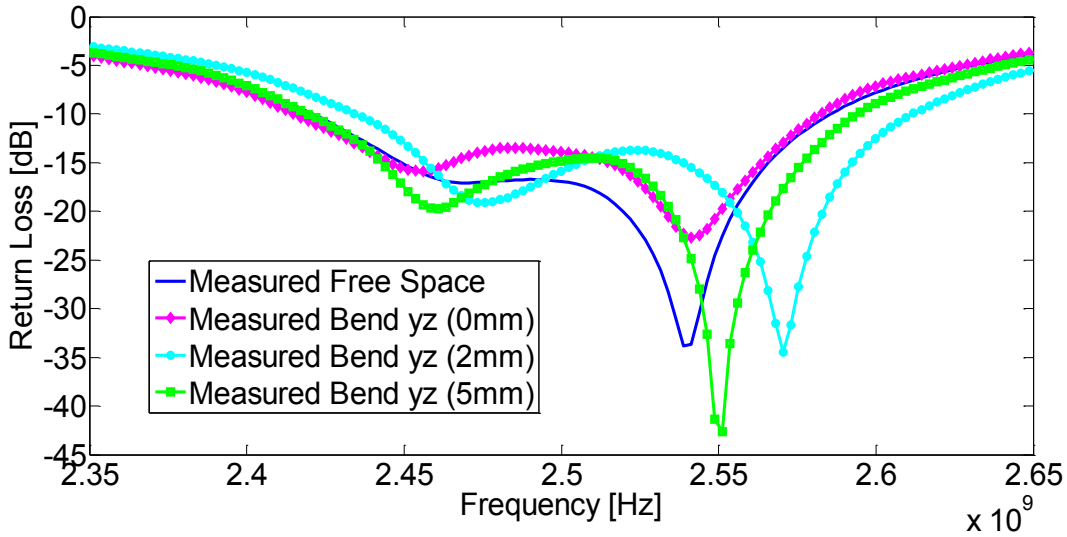

Figure 7.5 *Variation in Return Loss with Bending in yz-plane on the Arm.*

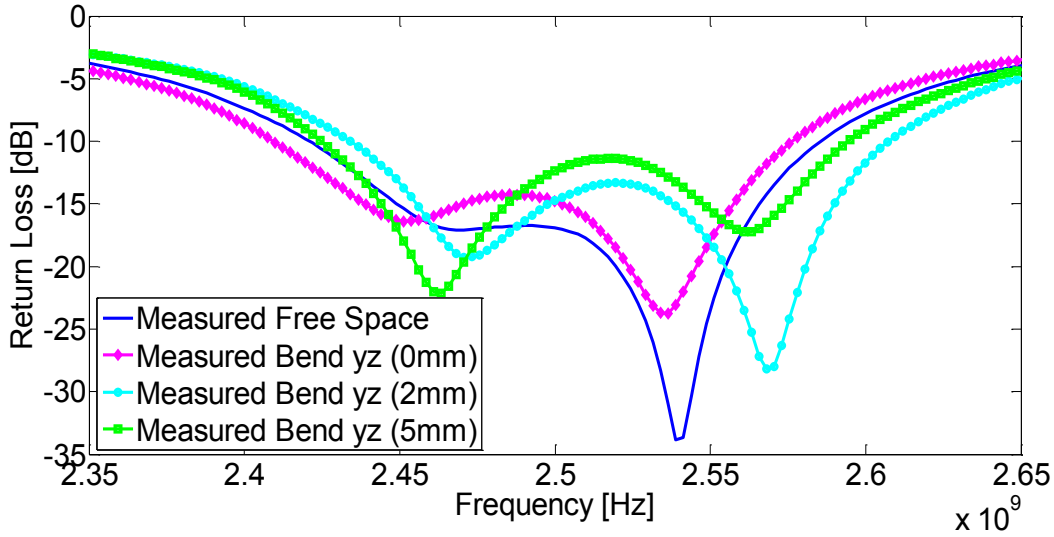

Figure 7.6 *Variation in Return Loss with Bending in yz-plane on the Leg.*

Table 7.3 tabulates the variation in return loss for different bending conditions along the yz-plane with -10 dB criteria of return loss.

Table 7.3 *Return Loss and Impedance Bandwidth in Bending along the yz-plane.*

Antenna Position		Return Loss at 2.45 GHz	Bandwidth [MHz] (-10 dB criteria)
Arm	0 mm	-15.45	168 (2.418 – 2.586)
	2 mm	-12.65	164 (2.437 – 2.601)
	5 mm	-17.11	173 (2.420 – 2.593)
Leg	0 mm	-16.27	165 (2.411 – 2.576)
	2 mm	-13.00	172 (2.436 – 2.608)
	5 mm	-16.84	168 (2.426 – 2.594)

Table 7.4 tabulates the antenna gain near human body with varying distance at 2.45 GHz. For simulation, the model presented in [36] is used with the properties of skin, fat and muscles at 2.45 GHz [35].

Table 7.4 *Antenna Gain Near Human Body.*

Antenna Position	Simulated [dB]	Measured [dB]
0 mm	2.49	3.07
2 mm	2.46	2.83
5 mm	2.41	2.28

Figure 7.7 shows the rectangular plot of simulated and measured near body radiation pattern at 2.45 GHz. The main purpose of using the rectangular plot instead of the polar plot is to show the difference in the simulated and measured results clearly as in the polar plot the negative values are also included which makes the analysis difficult to be done.

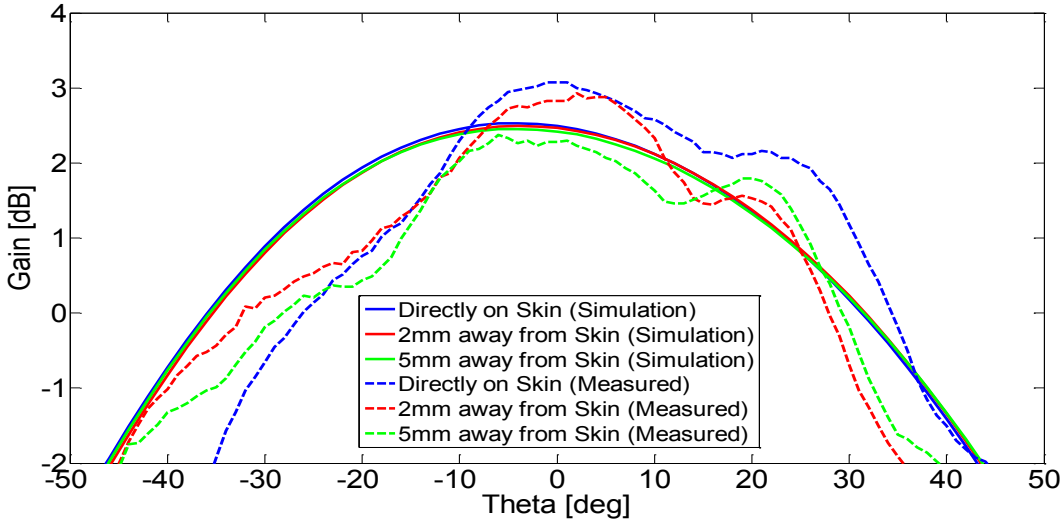

Figure 7.7 *Antenna Radiation Pattern near Human Body.*

7.4 On-body Measurements of EPDM Antenna

To have a better understanding, bending of the EPDM antenna is done in both xz-plane and yz-plane on leg and arm of a male.

7.4.1 Bending of EPDM Antenna in xz-plane

Figure 7.8 shows the antenna's position during bending measurements in xz-plane.

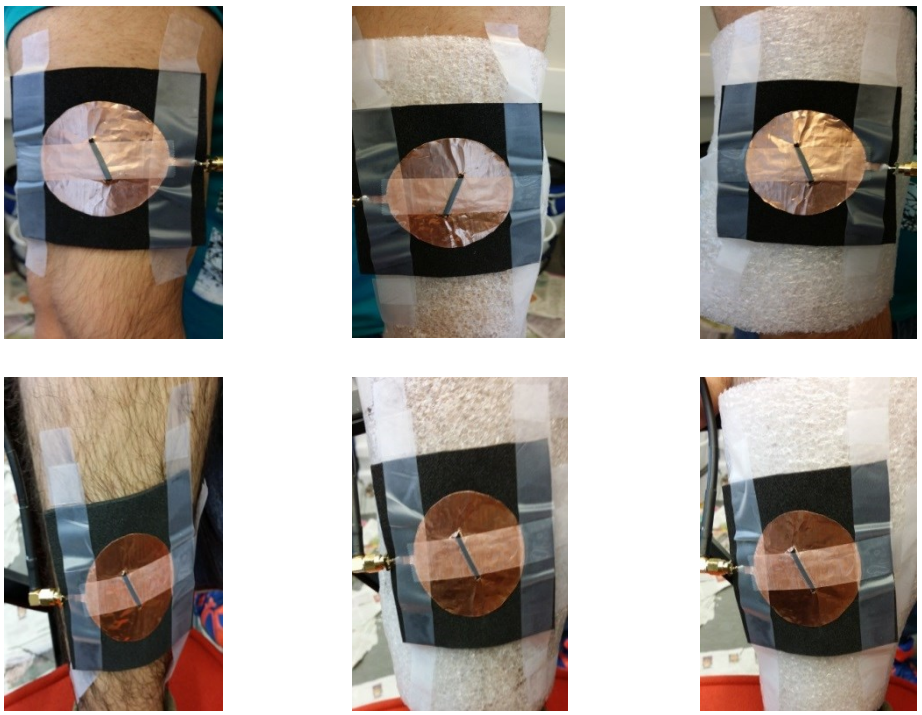

Figure 7.8 *Bending of EPDM Antenna in xz-plane*

Figure 7.9 and Figure 7.10 show the variation of return loss on the arm and the leg in bending conditions along the xz-plane. Even in case of EPDM, the near body results show larger bandwidth compared with the measured free space results. The return loss has significantly decreased but the antenna still operates on 2.45 GHz in all cases of bending in xz-plane. The operating frequency band is shifted towards lower frequencies due to larger electrical length when the antenna is in the vicinity of the human body.

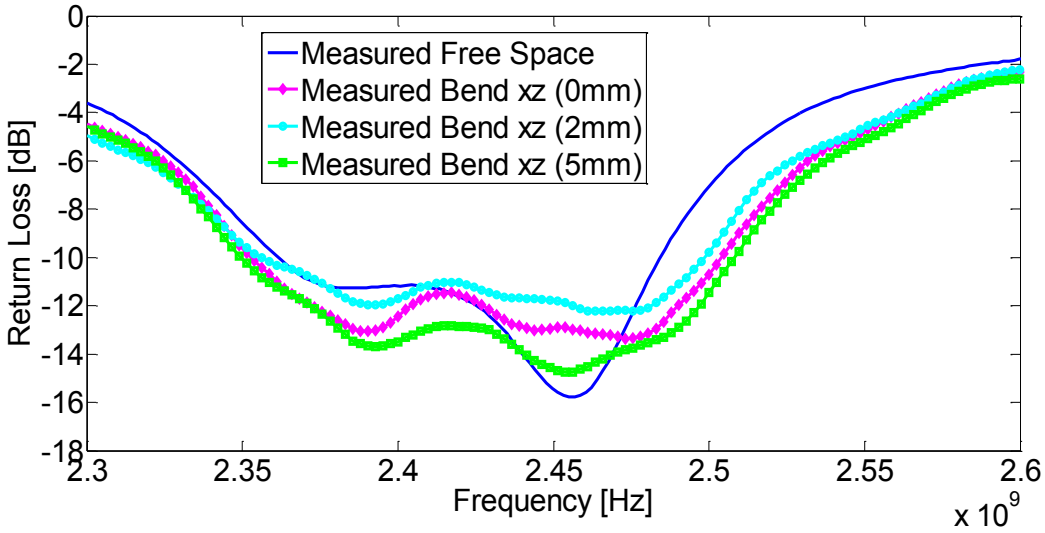

Figure 7.9 *Variation in Return Loss with Bending in xz-plane on the Arm.*

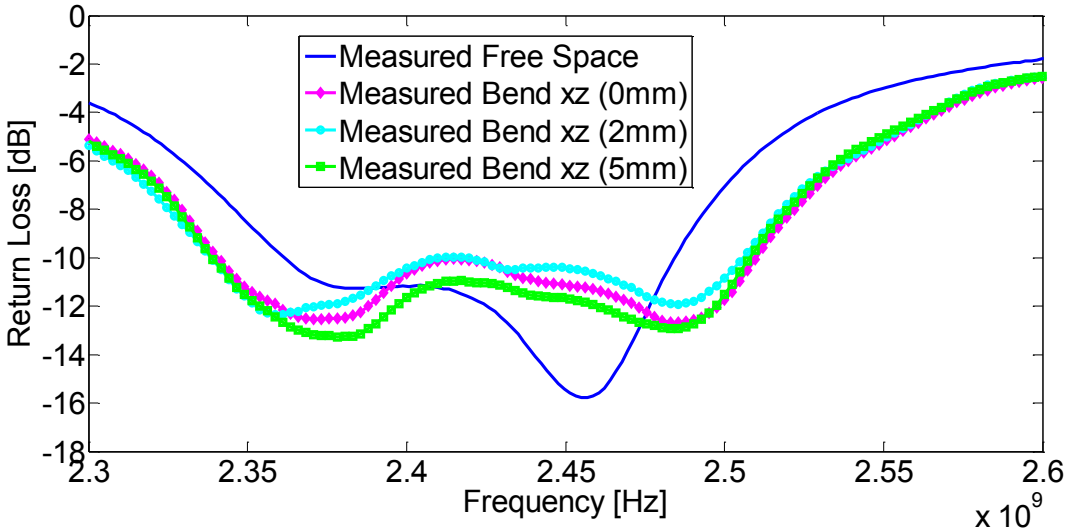

Figure 7.10 *Variation in Return Loss with Bending in xz-plane on the Leg.*

Table 7.5 tabulates the variation in return loss for different bending conditions in the xz-plane with -10 dB criteria of return loss.

Table 7.5 *Return Loss and Impedance Bandwidth in Bending along the xz-plane.*

Antenna Position		Return Loss at 2.45 GHz	Bandwidth [MHz] (-10 dB criteria)
Arm	0 mm	-12.96	149 (2.354 GHz – 2.503 GHz)
	2 mm	-11.75	141 (2.357 GHz – 2.498 GHz)
	5 mm	-14.55	152 (2.352 GHz – 2.504 GHz)
Leg	0 mm	-11.11	168 (2.342 GHz – 2.510 GHz)
	2 mm	-10.40	166 (2.340 GHz – 2.506 GHz)
	5 mm	-11.65	168 (2.340 GHz – 2.508 GHz

7.4.2 Bending of EPDM Antenna in yz-plane

Figure 7.11 shows the antenna's position during bending measurements in yz-plane.

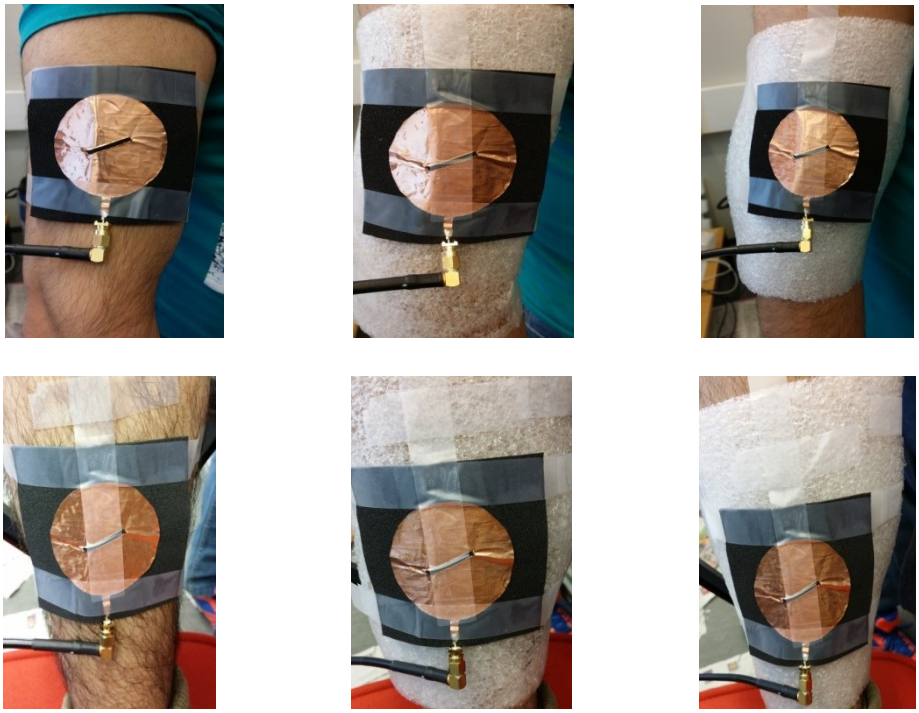

Figure 7.11 *Bending of EPDM Antenna in yz-plane.*

Figure 7.12 and Figure 7.13 show the variation of return loss on the arm and the leg in bending conditions along the yz-plane. The near body results show that in bending conditions along the yz-plane, the resonant frequency shifts to higher bands as well as the return loss degrades. Considering the -6 dB criteria for return loss [37][38], the antenna operates for 2.45 GHz in all bent conditions.

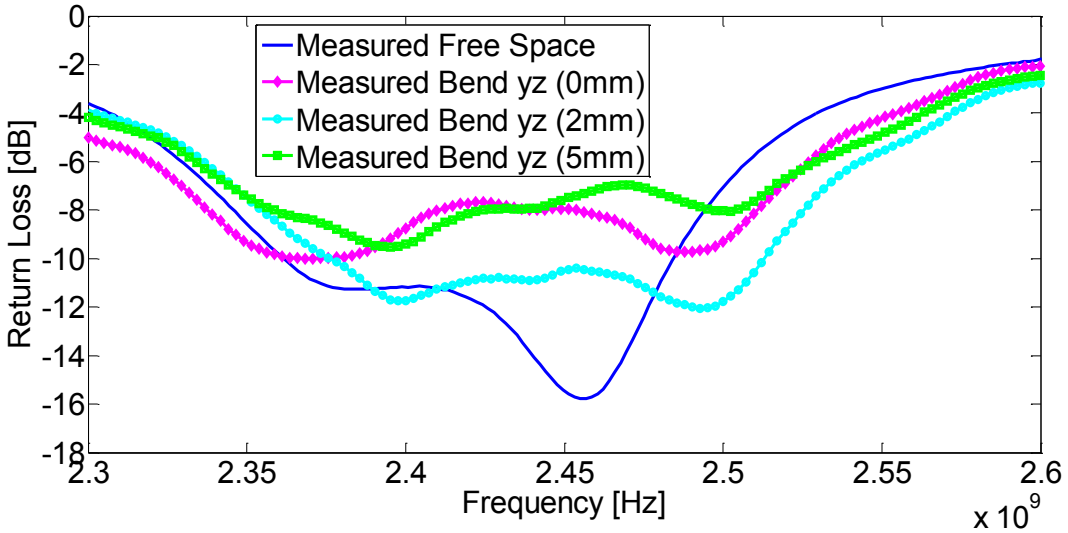

Figure 7.12 *Variation in Return Loss with Bending in yz-plane on the Arm.*

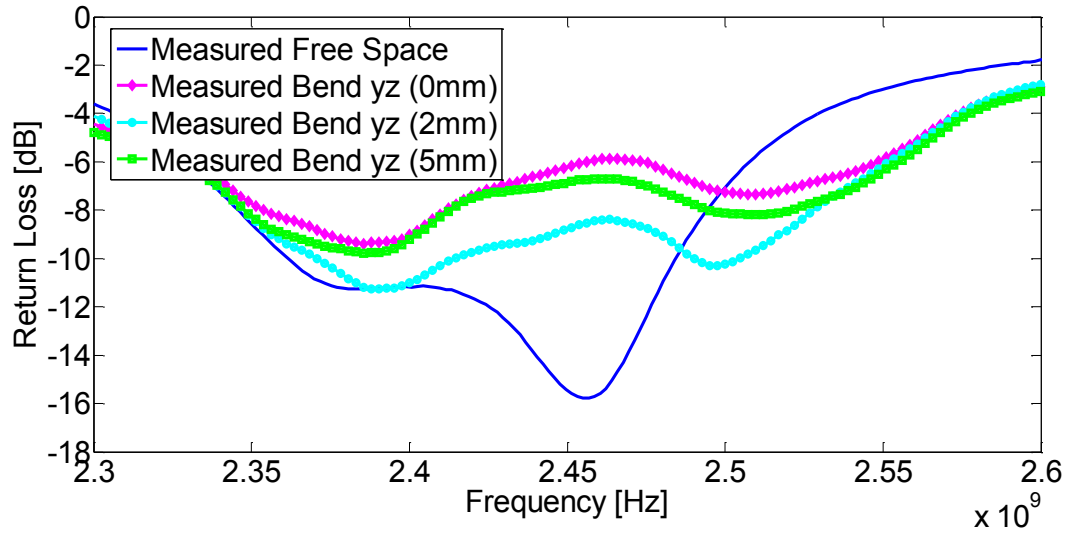

Figure 7.13 *Variation in Return Loss with Bending in yz-plane on the Leg.*

Table 7.6 tabulates the variation in return loss for different bending conditions in the yz-plane with -6 dB criteria of return loss.

Table 7.6 *Return Loss and Impedance Bandwidth in xz-plane Bending.*

Antenna Position		Return Loss at 2.45 GHz	Bandwidth [MHz] (-6 dB criteria)
Arm	0 mm	-7.95	208 (2.320 GHz – 2.528 GHz)
	2 mm	-10.53	135 (2.379 GHz – 2.514 GHz)
	5 mm	-7.61	195 (2.335 GHz – 2.530 GHz)
Leg	0 mm	-6.25	212 (2.335 GHz – 2.547 GHz)
	2 mm	-8.83	216 (2.333 GHz – 2.549 GHz)
	5 mm	-6.88	224 (2.330 GHz – 2.554 GHz)

Table 7.7 tabulates the simulated and measured gain in the main radiation beam at 2.45 GHz with varying distance with the human body. For simulation, the model presented in [36] is used with the properties of skin, fat and muscles at 2.45 GHz [35].

Table 7.7 *Antenna Gain near Human Body.*

Antenna Position	Simulated [dB]	Measured [dB]
0 mm	7.29	7.21
2 mm	7.16	6.82
5 mm	7.09	5.43

Figure 7.14 shows the rectangular plot of simulated and measured near body radiation pattern at 2.45 GHz. The main purpose of using the rectangular plot instead of the polar plot is to show the difference in the simulated and measured results clearly as in the polar plot the negative values are also included which make the analysis difficult. For the frequencies above 1 GHz, the antenna gain is increased due to low penetration depth and reflections from the human body [39][40]. This phenomenon can be clearly seen in Figure 7.14 for both simulated and measured near body radiation patterns in xz-plane.

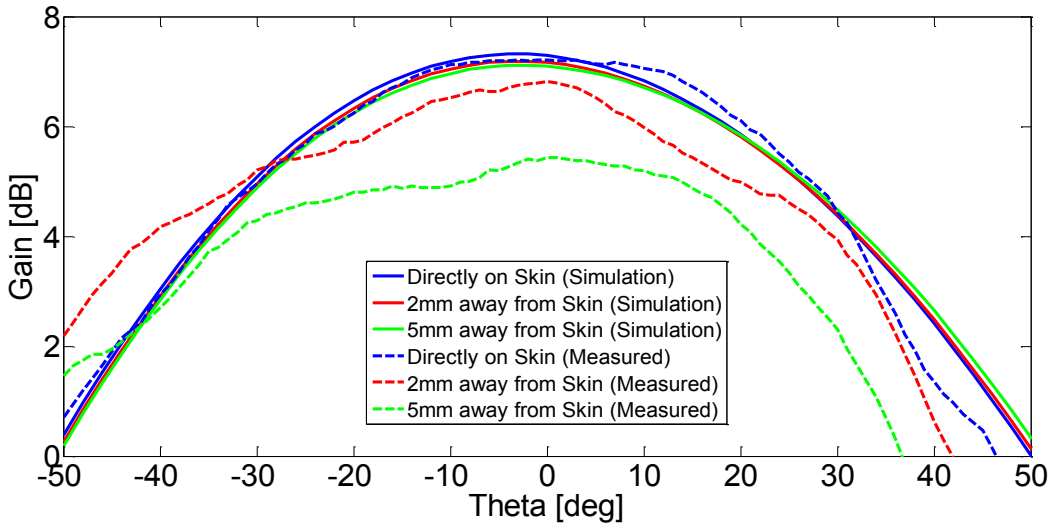

Figure 7.14 *Antenna Radiation Pattern near Human Body.*

8. CONCLUSION AND FUTURE WORK

This chapter concludes the thesis, highlights the main results, and proposes the future work that can be done related to the research.

8.1 Conclusion

In this Master's thesis, the performance evaluation of wearable antennas using different flexible substrates has been discussed. For this purpose, two circularly polarized microstrip patch antennas were designed on Denim and EPDM foam substrate. To achieve circular polarization a rectangular slot along the diagonal axis is inserted at the center of the circular patch. In order to evaluate the performance, both free space and on-body results were analysed. Finally, a set of comparative results of the antenna in free space and different body parts like arm and leg are compared to validate the operability of the antenna in real environment.

The antenna's analysis showed good agreement between simulated and measured free space results, however due to fabrication inaccuracies, some shifting of operating frequency is observed. Free space bending is analysed in two planes i.e. xz and yz, with two different bending radii (50 mm and 75 mm). Bending analysis showed that the performance of the antenna is affected more when the antenna is bent along the direction which determines its resonance length. Impedance matching is improved when the antenna is bent in the xz-plane. Beam width increases in the plane of bending which results in decreased antenna gain.

The near body performance of the designed antennas is analyzed by varying the distance between the antenna and the human body using a polyethylene foam sheet of different thicknesses. Three different distances were selected, i.e. 0 mm (directly on skin), 2 mm and 5 mm, to have a better idea of the effects with respect to varying distance between the human body and the wearable antenna. The performance of the antenna in terms of the input matching and the impedance bandwidth is analyzed on two different body parts, i.e. arm and leg, with bending in both xz-plane and yz-plane. The results show a decrease in return loss due to the lossy nature of the human body, and increase in bandwidth due to the lowering of the Q factor of the antenna. The antenna gain is increased due to low penetration depth and reflections from the human body in simulation and real on-body measurements at high frequencies. The percentage increase in gain near human body for EPDM and Denim is around 19.56 % and 10.66 % respectively.

The summary of results shows that the designed antennas operate for the desired frequency bands with good efficiency in all simulated and measured scenarios; however EPDM antenna is better in terms of antenna impedance and radiation characteristics, weight, wearing comfort, and can naturally and forcibly retract to its original dimensions after deformation.

8.2 Future Work

The copper tape used in the fabrication of the antenna is not very reliable. It peels off or breaks when the antenna is bent. This makes the antenna less durable and can fail the communication system. Figure 8.1 shows the broken and peeled off copper tape on the Denim antenna.

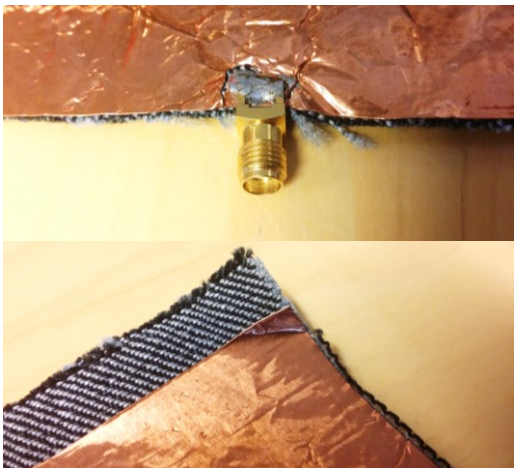

Figure 8.1 *Problems in Copper Tape.*

To avoid this, the antenna can be fabricated using new printable technologies where conductive part is printed on the substrate. Currently used printable technologies include Inkjet and 3D Printing. In these technologies, conductive inks are used to print the desired pattern on substrate using either the Inkjet or Micro Dispense 3D Printer, and then sintered to produce a solid conductive track. Figure 8.2 shows the Inkjet or Micro Dispense 3D Printer.

(a) (b)

Figure 8.2 *Printers (a) Inkjet (b) Micro Dispense 3D.*

9. PUBLICATIONS

- "Circularly Polarized Textile Antenna For 2.45 GHz", Muhammad Rizwan, Yahya Rahmat-Samii and Leena Ukkonen, IEEE International Microwave Workshop Series on RF and Wireless Technologies for Biomedical and Healthcare Applications (IMWS-Bio 2015).

- "Impact of Bending on The Performance of Circularly Polarized Wearable Antenna", Muhammad Rizwan, Lauri Sydänheimo, and Leena Ukkonen, The 36th Progress In Electromagnetics Research Symposium (PIERS 2015).

- "Performance Evaluation of Circularly Polarized Patch Antenna on Flexible EPDM Substrate Near Human Body", Muhammad Rizwan, M. Waqas A. Khan, Lauri Sydänheimo and Leena Ukkonen, The 11th Loughborough Antennas and Propagation Conference (LAPC 2015).

REFERENCES

[1] J. G. Santas, A. Alomainy and Yang Hao, “Textile Antennas for On-Body Communications: Techniques and Properties”, The Second European Conference on Antennas and Propagation (EuCAP), pp. 1-4, Nov. 2007.

[2] B. Y. Toh, R. Cahill, and V. F. Fusco, “Understanding and measuring circular polarization”, IEEE Trans. Ed, vol. 46, pp. 313-318, Aug. 2003.

[3] Yazdandoost, Kamya Yekeh, and Ryu Miura, “Antenna polarization mismatch in BAN communications”, IEEE IMWS-BIO, pp. 1-3, Dec. 2013.

[4] Abdulrahman Shueai Mohsen Alqadami, M.F. Jamlos, “Design and development of a flexible and elastic UWB wearable antenna on PDMS substrate”, IEEE APACE, pp. 27-30, Dec. 2014.

[5] E. F. Sundarsingh et al., “Polygon-shaped slotted dual-band antenna for wearable applications,” IEEE Antennas Wireless Propag. Lett., vol. 13, pp. 611-614, 2014.

[6] J.D. Kraus, D.A. Fliesch, “Electromagnetics with Applications”, 5th Edition, USA, McGraw-Hill. 1999.

[7] D.M. Pozar, “Microwave Engineering”, USA, Addison-Wesley Publishing Company. 1990. 719 p.

[8] J.D. Kraus, “Antennas for All Applications”, 3rd Edition, USA, McGraw-Hill. 2002. 921 p.

[9] Warren L. Stutzman, Gary A. Thiele, “Antenna theory and design”, 2nd ed., John Wiley & Sons, Inc. 1998.

[10] IEEE Standard Definitions of Term for Antennas, IEEE Standard 145-1993, IEEE: 445-199 Hoes Lane, Piscataway, NJ, 1993.

[11] Constantine A. Balanis, “Antenna Theory: Analysis and Design”, 3rd ed., John Wiley & Sons, Inc. 2005.

[12] Peter S. Hall and Yang Hao, “Antennas and Propagation for Body-Centric Wireless Communications”, Artech House, Inc. MA, 2006.

[13] B. Latre, B. Braem, I. Moennan, C. Blondia, and P. Demeester, “A survey on wireless body area networks”, Journal of Wireless Networks, vol. 17, pp. 1-18, 2011.

[14] P. Salonen, L. Sydanheimo, M. Keskilammi and M. Kivikoski, “A small planar inverted-F antenna for wearable applications”, The Third International Symposium on the Wearable Computers, pp. 95-100, 1999.

[15] P. Massey, “Mobile phone fabric antennas integrated within clothing”, International Conference on Antennas and Propagation, vol. 1, pp. 344-347, Apr. 2001.

[16] P. Salonen and L. Sydanheimo, “Development of an S-band flexible antenna for smart clothing”, International Symposium on Antennas and Propagation, vol. 3, pp. 6-9, 16-21 Jun. 2002.

[17] P. Salonen and L. Hurme, “A novel fabric WLAN antenna for wearable applications”, International Symposium on Antennas and Propagation, vol. 2, pp. 700-703, 22-27 Jun. 2003.

[18] M. Tanaka and J. Jae-Hyeuk, “Wearable microstrip antenna,” International Symposium on Antennas and Propagation, vol. 2, pp. 704-707, 22-27 Jun. 2003.

[19] C. Cibin, P. Leuchtmann, M. Gimersky, R. Vahldieck, and S. Moscibroda, “A flexible wearable antenna”, International Symposium on Antennas and Propagation, vol. 4, pp. 3589-3592, 20-25 Jun. 2004.

[20] A. Jafargholi, “VHF-LB Vest Antenna Design”, International Workshop on Antenna Technology: Small and Smart Antennas Metamaterials and Applications, pp. 247-250, 21-23 Mar. 2007.

[21] P. Salonen, Y. Rahmat-Samii and M. Kivikoski, “Wearable antennas in the vicinity of human body”, International Symposium on Antennas and Propagation Society, vol. 1, pp. 467-470, 20-25 Jun. 2004.

[22] M. Klemm, I. Locher and G. Troster, “A novel circularly polarized textile antenna for wearable applications”, 7th European Conference on Wireless Technology, pp. 285-288, 11-12 Oct. 2004.

[23] A. Tronquo, H. Rogier, C. Hertleer and L. Van Langenhove, “Robust planar textile antenna for wireless body LANs operating in 2.45 GHz ISM band”, Electron. Lett., vol. 42, pp. 21-22, 2006.

[24] C. Hertleer, H. Rogier, L. Vallozzi and F. Declercq, “A Textile Antenna based on High-Performance Fabrics”, The Second European Conference on Antennas and Propagation, pp. 1-5, 11-16 Nov. 2007.

[25] C. Hertleer, H. Rogier and L. Van Langenhove, “A Textile Antenna For Protective Clothing”, IET Seminar on Antennas and Propagation for Body-Centric Wireless Communications, pp. 44-46, 24 Apr. 2007.

[26] C. Hertleer, H. Rogier, L. Vallozzi, L. Van Langenhove, "A Textile Antenna for Off-Body Communication Integrated Into Protective Clothing for Firefighters", IEEE Transactions on Antennas and Propagation, vol. 57, no. 4, pp. 919-925, Apr. 2009.

[27] E. Kaivanto, J. Lilja, M. Berg, E. Salonen, P. Salonen, "Circularly polarized textile antenna for personal satellite communication", The Fourth European Conference on Antennas and Propagation, pp. 1-4, 12-16 Apr. 2010.

[28] Yazdandoost, Kamya Yekeh, and Ryu Miura. "Antenna polarization mismatch in BAN communications", IEEE IMWS-BIO, pp. 1-3, Dec. 2013.

[29] Ismail, Muhammad Faizal, et al. "Compact circularly polarized textile antenna" IEEE ISWTA, pp. 134-136, 2014.

[30] ANSYS HFSS, Available at: http://www.ansys.com/Products/Simulation+Technology/Electronics/Signal+Integrity/ANSYS+HFSS

[31] Reddy, Gopi Shrikanth, et al. "High gain and low cross-polar compact printed elliptical monopole UWB antenna loaded with partial ground and parasitic patches", Progress In Electromagnetics Research, vol. 43, pp. 151-167, 2012.

[32] A. Samsuri, "An Introduction to Polymer Science and Rubber Technology", University Publication Centre (UPENA), Universiti Teknologi MARA 2009.

[33] N.A.L. Alias, N.A.M. Affendi, Z. Awang, M.T. Ali, A. Samsuri, "Preliminary studies on the use of natural rubber in the design of flexible microstrip antennas", IEEE International RF and Microwave Conference (RFM), pp. 454-459, 9-11 Dec. 2013.

[34] K. Oohira, "Development of an antenna material based on rubber that has flexibility and high impact resistance", NTN Technical Rev., no.76, 2008.

[35] Dielectric properties of body tissues. Available at: http://niremf.ifac.cnr.it/tissprop/

[36] S. Shahid, M. Rizwan, M.A.B. Abbasi, H. Zahra, S.M. Abbas, M.A. Tarar, "Textile antenna for body centric WiMAX and WLAN applications", International Conference on Emerging Technologies (ICET), pp. 1-5, 8-9 Oct. 2012.

[37] J. Rocas, N. Pires, A.A Moreira, "Human body effects on the matching of a 2.45 GHz coplanar-fed antenna", 7th European Conference on Antennas and Propagation (EuCAP), pp. 3279-3281, 8-12 Apr. 2013.

[38] J.S. Bellon et al., “Textile MIMO antenna for Wireless Body Area Networks”, 5th European Conference on Antennas and Propagation (EUCAP), pp. 428-432, 11-15 Apr. 2011.

[39] A. Alomainy, Y. Hao and F. Pasveer, “Modelling and characterization of a compact sensor antenna for healthcare applications”, 4th International workshop on Wearable and Implantable Body Sensor Networks (IFMBE), vol. 13, pp. 3-8, 2007.

[40] Zhi Ning Chen, “Antennas for Portable Devices”, 1st ed. John Wiley & Sons, Inc. 2007.